The Apoplastic Copper AMINE OXIDASE1 Mediates Jasmonic Acid-Induced Protoxylem Differentiation in Arabidopsis Roots[1]

Sandip A. Ghuge[2], Andrea Carucci, Renato A. Rodrigues-Pousada, Alessandra Tisi, Stefano Franchi, Paraskevi Tavladoraki, Riccardo Angelini, and Alessandra Cona*

Dipartimento di Scienze, Università degli Studi Roma Tre, 00146 Rome, Italy (S.A.G., A.Ca., A.T., S.F., P.T., R.A., A.Co.); Department of Life, Health, and Environmental Sciences, Università dell'Aquila, 67100 L'Aquila, Italy (R.A.R.-P.); and Istituto Nazionale Biostrutture e Biosistemi, 00136 Rome, Italy (P.T., R.A., A.Co.)

ORCID ID: 0000-0002-1399-1187 (R.A.).

Polyamines are involved in key developmental processes and stress responses. Copper amine oxidases oxidize the polyamine putrescine (Put), producing an aldehyde, ammonia, and hydrogen peroxide (H_2O_2). The Arabidopsis (*Arabidopsis thaliana*) amine oxidase gene At4g14940 (*AtAO1*) encodes an apoplastic copper amine oxidase expressed at the early stages of vascular tissue differentiation in roots. Here, its role in root development and xylem differentiation was explored by pharmacological and forward/reverse genetic approaches. Analysis of the *AtAO1* expression pattern in roots by a promoter::green fluorescent protein-β-glucuronidase fusion revealed strong gene expression in the protoxylem at the transition, elongation, and maturation zones. Methyl jasmonate (MeJA) induced *AtAO1* gene expression in vascular tissues, especially at the transition and elongation zones. Early protoxylem differentiation was observed upon MeJA treatment along with Put level decrease and H_2O_2 accumulation in wild-type roots, whereas *Atao1* loss-of-function mutants were unresponsive to the hormone. The H_2O_2 scavenger *N*,*N*^{1}-dimethylthiourea reversed the MeJA-induced early protoxylem differentiation in wild-type seedlings. Likewise, Put, which had no effect on *Atao1* mutants, induced early protoxylem differentiation in the wild type, this event being counteracted by *N*,*N*^{1}-dimethylthiourea treatment. Consistently, *AtAO1*-overexpressing plants showed lower Put levels and early protoxylem differentiation concurrent with H_2O_2 accumulation in the root zone where the first protoxylem cells with fully developed secondary wall thickenings are found. These results show that the H_2O_2 produced via AtAO1-driven Put oxidation plays a role in MeJA signaling leading to early protoxylem differentiation in root.

Root development is affected by several environmental stresses that may result in the inhibition of root growth and/or the modulation of differentiation pattern. It is not surprising, then, that a complex network of hormonal signals control root architecture under either physiological or stress growth conditions, since in changing environments plants take advantage of root developmental plasticity. Thus, it is reasonable that root growth and vascular development can be either conveniently coordinated or selectively modulated in growing roots depending on specific plant needs, in order to ensure the appropriate water absorption and nutrient uptake in heterogenous soils with varying resource availability.

During root vascular development, pericycle/vascular meristematic stem cells differentiate into procambial cell lineages, including protoxylem and metaxylem, intervening procambium, phloem, and pericycle (Mähönen et al., 2006; Petricka et al., 2012). Coordinated events of secondary cell wall deposition and programmed cell death (PCD) characterize the last stage of both protoxylem and metaxylem vessel maturation (Ohashi-Ito and Fukuda, 2010). It is well known that, under physiological conditions, an array of auxin, cytokinin, and brassinosteroid signaling pathways participate in root tissue differentiation (Petricka et al., 2012; Mähönen et al., 2014). Specifically, it has been proposed that vascular patterning is finely regulated by a feedback loop between auxin and cytokinin signaling pathways occurring through mutual inhibition (Bishopp et al., 2011; Perilli et al., 2012; Petricka et al., 2012). Brassinosteroids have also been shown to induce root growth and promote xylem differentiation by driving the entry of xylem precursors into the final stage of tracheary element differentiation (Yamamoto et al., 1997). Recently, reactive oxygen species (ROS) have been described to

[1] This work was supported by European COST Action COSTFA0605, the Italian Ministry of Education, University, and Research (project no. PRIN 2009WTCJL8_003), and the Università degli Studi Roma Tre, Italy.

[2] Present address: Institute of Crystallography, Italian National Research Council, 00015 Monterotondo, Italy.

* Address correspondence to alessandra.cona@uniroma3.it.

The author responsible for distribution of materials integral to the findings presented in this article in accordance with the policy described in the Instructions for Authors (www.plantphysiol.org) is: Alessandra Cona (alessandra.cona@uniroma3.it).

S.A.G., A.Ca., and A.T. designed and performed the research; S.F. performed the research; R.A.R.-P., R.A., and A.Co. designed the research; P.T. and A.Co. analyzed the data; R.A.R.-P., R.A., and A.Co. wrote the article.

www.plantphysiol.org/cgi/doi/10.1104/pp.15.00121

play a key role in the transition from cell proliferation to tissue differentiation in the root (Tsukagoshi et al., 2010), independently from the auxin/cytokinin feedback loop mentioned above. Indeed, while superoxide anion is required to maintain cell proliferation in the meristem, hydrogen peroxide (H_2O_2) is required for tissue differentiation in the elongation/differentiation zone.

However, less attention has been devoted to xylem differentiation under stress growth conditions, when resource availability and/or water supply may be restrictive, creating the need for a rearrangement of root architecture and vascular differentiation. In this regard, an alteration of the temporal pattern of xylem differentiation was observed in roots of soybean (*Glycine max*) plants upon saline stress, with a delay in primary xylem differentiation and a precocious formation of secondary xylem (Hilal et al., 1998). Moreover, significant anatomical changes were observed to occur in roots of *Agave salmiana* under water stress, among them a reduction of vessel number and an increase of xylem diameter and wall thickness (Peña-Valdivia and Sánchez-Urdaneta, 2009). The rearrangement of root vascular tissues has also been reported to occur as a defense reaction against pathogen invasion, such as the regeneration of xylem vessels observed in a *Fusarium* spp. wilt-resistant carnation (*Dianthus caryophyllus* 'Novada') upon fungal infection to compensate for local vascular dysfunction (Baayen, 1986) as well as the vascular tissue redifferentiation revealed in Arabidopsis (*Arabidopsis thaliana*) plants following nematode invasion in order to counteract mechanical pressure (Møller et al., 1998). Moreover, xylem regeneration around a wound has been described in maize (*Zea mays*) seedling stems (Aloni and Plotkin, 1985).

Of note, previous studies reported that the stress signaling hormone jasmonic acid (JA), while inducing root growth inhibition (Ren et al., 2009), behaves as a promoter of early vascular tissue differentiation (Cenzano et al., 2003) and xylogenesis (Fattorini et al., 2009). The role of JA in vascular tissue differentiation was first revealed in stolons of potato (*Solanum tuberosum*) during the tuberization process. In particular, exogenous JA accelerated potato tuber formation via the induction of both cell expansion and early differentiation of protoxylem vessels with ring-shaped secondary wall thickenings, leading to increased movement of nutrients toward the stolon tip (Cenzano et al., 2003). Moreover, exogenous methyl jasmonate (MeJA) was reported to enhance the formation of adventitious roots and the development of xylogenic nodules in tobacco (*Nicotiana tabacum*) thin layers under root-inductive hormonal conditions (Fattorini et al., 2009).

The polyamines (PAs) putrescine (Put), spermidine (Spd), and spermine (Spm) are small aliphatic polycations ubiquitous in living organisms and essential for cell growth, proliferation, and differentiation (Tavladoraki et al., 2012). In plants, PAs have been involved in a multiplicity of developmental processes as well as stress responses and tolerance strategies, their intracellular and extracellular levels varying in response to different physiological and pathological conditions (Mattoo et al., 2010). A fine regulation of their metabolism and/or transport ensures the occurrence of the appropriate PA levels depending on the specific cell needs (Tavladoraki et al., 2012). Oxidative deamination of PAs is catalyzed by amine oxidases (AOs) in a multistep mechanism, with the release of the removed amine moiety and amino aldehydes in the oxidative phase and the production of H_2O_2 in the reoxidation step of the reduced enzyme (Tavladoraki et al., 2012). Although AOs are a heterogenous class of enzymes varying in subcellular localization, tissue expression pattern, substrate specificity, and mode of catalysis, they share roles in both the homeostasis of PAs and the production of H_2O_2, the latter representing a common product in the AO-driven oxidative catabolism of PAs (Cona et al., 2006; Tavladoraki et al., 2012). On the basis of the cofactor involved, AOs can be classified into two subclasses: the copper amine oxidases (CuAOs), showing high affinity for Put, and the FAD-dependent polyamine oxidases (PAOs), whose preferred substrates are Spd, Spm, and/or their acetyl derivatives (Cona et al., 2006; Tavladoraki et al., 2012). In Arabidopsis, five *PAO* genes (*AtPAOs*) and 10 *CuAO* genes (*AtCuAOs*) were identified by database search and in some cases characterized at the protein level (Fincato et al., 2011; Planas-Portell et al., 2013; Ahou et al., 2014; Kim et al., 2014). Among *CuAO* genes, At4g14940 (The Arabidopsis Information Resource [TAIR] accession no. 2129519), here designed as *AtAO1* (formerly *ATAO1*; Møller and McPherson, 1998), encodes an extracellular protein found in apoplastic fluids of Arabidopsis rosettes, as demonstrated by mass spectrometry analysis (Boudart et al., 2005).

H_2O_2 derived from the extracellular catabolism of PAs by cell wall-localized AOs has been shown to be involved in both developmental processes, such as the light-induced inhibition of mesocotyl growth (Cona et al., 2003) and the PCD occurring in differentiating tracheary elements (Tisi et al., 2011b), as well as defense responses during wound healing (Angelini et al., 2008), salt stress (Moschou et al., 2008), and pathogen attack (Moschou et al., 2009). In this regard, *AOs* have also been suggested to act as stress-responsive genes whose expression strongly increases in response to both pathogen infection and abiotic stresses (Moschou et al., 2008; Tavladoraki et al., 2012). During the plant response to stresses, a faster apoplastic oxidation of PAs has been supposed to occur, allowed by the concurrent increase of PA secretion and catabolism in the cell wall, and the PA-derived H_2O_2 has been demonstrated to trigger signal transduction pathways leading to the induction of defense gene expression, stress tolerance, or PCD (Moschou et al., 2008; Tisi et al., 2011a). Recently, the dual role of PAs as either signaling compounds or the source of the second messenger H_2O_2 has been highlighted, and it has been hypothesized that AOs may have a role in PA/H_2O_2 balance (Moschou et al., 2008; Tisi et al., 2011a, 2011b). In fact, the coordinated modulation of PA metabolism and secretion in the cell wall may represent a crucial mechanism in the control of the

PA-H_2O_2 ratio, which has been suggested to be a significant player in fixing cell fate and behavior under stress conditions (Moschou et al., 2008; Tisi et al., 2011a).

It is worth noting that the H_2O_2 derived from the apoplastic PA catabolism has been shown to be involved in JA-dependent wound signaling pathways, behaving as a mediator of cell wall-stiffening events during wound healing (Cona et al., 2006; Angelini et al., 2008). Moreover, it has been reported recently that PA-derived H_2O_2 inhibits root growth and promotes xylem differentiation, inducing both cell wall-stiffening events and developmental PCD (Tisi et al., 2011a, 2011b). Indeed, Spd treatment in maize or overexpression of maize PAO (ZmPAO) in the cell wall of tobacco plants induced early differentiation and precocious cell death of xylem precursors along with enhanced in vivo H_2O_2 production in xylem tissues of maize and tobacco root apex, respectively (Tisi et al., 2011a, 2011b). Owing to the high rate of apoplastic Spd catabolism supposed to occur upon Spd supply or PAO overexpression, it has been suggested that, in such unphysiological status, plants may experience stress-like conditions under which the AO-driven H_2O_2 production may have a role in promoting xylem differentiation (Tisi et al., 2011a).

Taking into account that *AtAO1* is expressed at the early stages of vascular tissue development in Arabidopsis roots (Møller et al., 1998; Møller and McPherson, 1998), we explored the possibility that the cell wall-localized AtAO1 could be involved in JA signaling, leading to the induction of root xylem differentiation by means of both pharmacological and forward/reverse genetic approaches. Our results show that *Atao1* loss-of-function mutants (TAIR accession nos. 1005841762 and 4284859) are unresponsive to MeJA signaling leading to root protoxylem differentiation. Conversely, AtAO1 overexpression leads to early protoxylem differentiation along with enhanced H_2O_2 production in the root zone where the first protoxylem cells with fully developed secondary wall thickenings can be observed. Overall, our data show that H_2O_2 produced via AtAO1-driven Put oxidation behaves as a mediator in JA-induced root xylem differentiation.

Moreover, the data presented here suggest that Put-derived H_2O_2 may play a role in xylem differentiation under stress growth conditions such as those signaled by MeJA or simulated by either Put treatment or AtAO1 overexpression.

RESULTS

The *AtAO1* Expression Pattern Is Associated with Xylem Tissues in the Root

We have analyzed *AtAO1* (TAIR accession no. 2129519) promoter activity in primary root using *AtAO1*::*GFP-GUS* Arabidopsis transgenic plants. Figure 1 shows that promoter-driven GUS expression was clearly visible in the vascular tissues at the division/differentiation transition zone (hereafter referred to as the transition zone) and the elongation zone as well as at the maturation zone, while some more tenuous expression was observed in older tissues (Fig. 1A). Expression was also strongly visible in root cap cells (Fig. 1A). Laser scanning confocal microscopy (LSCM) analysis of the *AtAO1* promoter-driven GFP signal confirmed the observations made with the GUS analysis but gave more detailed information. In the root apex zone, GFP signal extended basipetally from the immature protoxylem location in the transition zone toward the protoxylem cells with initial secondary wall thickenings (Fig. 1, B and D). Proceeding basipetally, the GFP signal was also detected in protoxylem cells at the final step of secondary cell wall thickening (Fig. 1, C and E), revealed as a sharp intensification of fluorescence upon PI staining as described below. GFP signal in this zone was also evident in the metaxylem precursors (Fig. 1E). The clear expression visible in the root apex (Fig. 1F) confirmed the GUS staining observation. At later developmental stages, the signal was no longer present in fully differentiated protoxylem cells, being then only associated with differentiating metaxylem precursors (Fig. 1G).

A more extensive study of *AtAO1* gene expression was carried out by analyzing root cross sections of 4-d-old seedlings. As shown in Figure 2, the spatial expression profile of *AtAO1* promoter-driven GUS staining along the primary root from the apex up to the maturation zones revealed the occurrence of promoter activity in both external and vascular tissues depending on tissue developmental stage. Initially, intense promoter activity was seen in the root cap (Fig. 2A) and in the outer tissues of the meristematic zone (Fig. 2, B–F). Proceeding basipetally from the transition zone toward the elongation (Fig. 2, F–H) and maturation (Fig. 2, I–L) zones, GUS staining was revealed in vascular tissues, more precisely in protoxylem precursors (Fig. 2, F–H), in the whole vascular cylinder (Fig. 2, I and J), and finally in metaxylem precursors (Fig. 2, K and L).

AtAO1 Expression in the Root Is Induced by MeJA

AO expression has been reported to be induced by exogenous JA and MeJA in several plant species (Cona et al., 2006; Angelini et al., 2008). Thus, the effect of MeJA at the concentrations of 0.1 and 50 μM on *AtAO1* expression levels was analyzed by reverse transcription-quantitative PCR (RT-qPCR) in 7-d-old Arabidopsis wild-type seedlings. Figure 3 shows that *AtAO1* expression level in whole seedlings increased after 1 h of treatment at both MeJA concentrations by 2- and 3.7-fold, respectively (Fig. 3A). The latter value is in agreement with the analysis of microarray data retrieved from the Arabidopsis eFP Browser (http://bar.utoronto.ca/efp/cgi-bin/efpWeb.cgi; Winter et al., 2007). Consistently, MeJA at both 0.1 μM (Fig. 3, C and F) and 50 μM (Fig. 3, D and G) considerably induced *AtAO1* promoter-driven GUS expression in roots of 4-d-old seedlings as compared with untreated control plants (Fig. 3, B and E), especially in the vascular tissues at the transition and elongation zones. In particular, upon

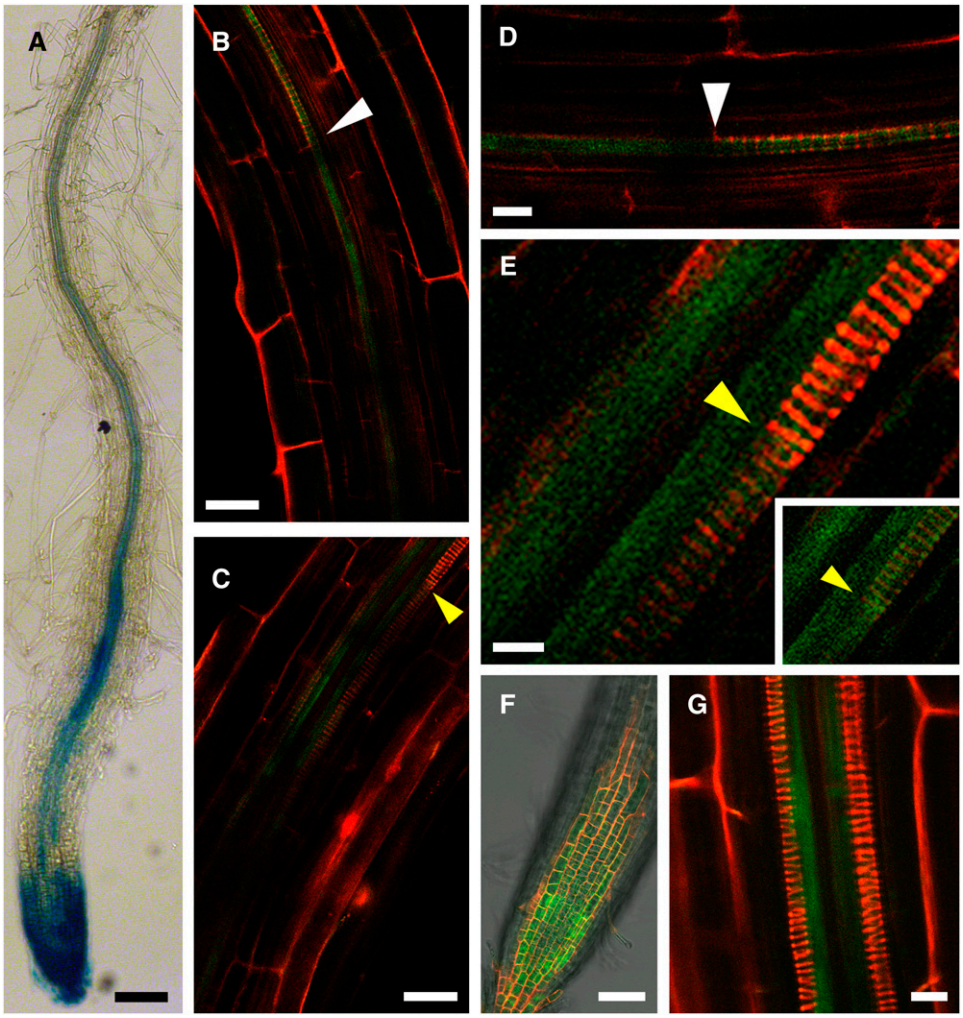

Figure 1. *AtAO1* tissue expression pattern in primary roots of 4-d-old *AtAO1*::*GFP-GUS* transgenic plants. A, Light microscopy analysis by GUS staining of the primary root terminal portion from the root cap up to approximately 2,000 μm from the apical meristem. The staining reaction was allowed to proceed overnight. B to G, LSCM analysis of GFP signal and propidium iodide (PI) staining. B, GFP signal in an immature protoxylem location and in protoxylem precursors with initial secondary cell wall thickenings (white arrowhead). C, GFP signal in protoxylem cells with fully developed secondary cell wall thickenings (yellow arrowhead). GFP signal is evident also at the immature metaxylem location. D, Magnification of the top field shown in B. E, Magnification of the top field shown in C. In the inset, the output levels of the red channel have been lowered in order to put in evidence the GFP green signal in differentiating protoxylem vessel. F, GFP signal in the root apex. G, Distal root zone showing GFP signal at the location of differentiating metaxylem precursors. Highly reproducible results were obtained from three independent transgenic lines. Micrographs are representative of those obtained from 25 roots from five independent experiments. Bars = 100 μm (A), 25 μm (B and C), 10 μm (D and G), 5 μm (E), and 50 μm (F).

treatment with 50 μM MeJA, a strongly intensified GUS staining was revealed in vascular tissues (Fig. 3, D and G), clearly detectable without interruption from the transition zone (immature protoxylem cells) up to the maturation zone (whole central cylinder). Otherwise, in the vascular tissues of control untreated plants, a weaker and discontinuous *AtAO1* expression pattern was observable, the signal being very faint and even absent ranging from the transition zone toward the initial portion of the maturation zone (Fig. 3, B and E). Interestingly, 0.1 μM MeJA also induced *AtAO1* expression, even if to a lower extent, revealing the occurrence of a spatial anticipation of the *AtAO1* expression pattern in the central cylinder (Fig. 3, C and F), evident from the transition zone up to the initial part of the maturation zone.

Atao1 Mutants Are Unresponsive to MeJA-Induced Early Protoxylem Differentiation in Roots

In order to investigate the physiological roles of AtAO1, two Salk transfer DNA (T-DNA) insertional mutant lines for the *AtAO1* gene (SALK_145639.55.25.X, TAIR accession no. 1005841762; and SALK_077391.40.85.X,

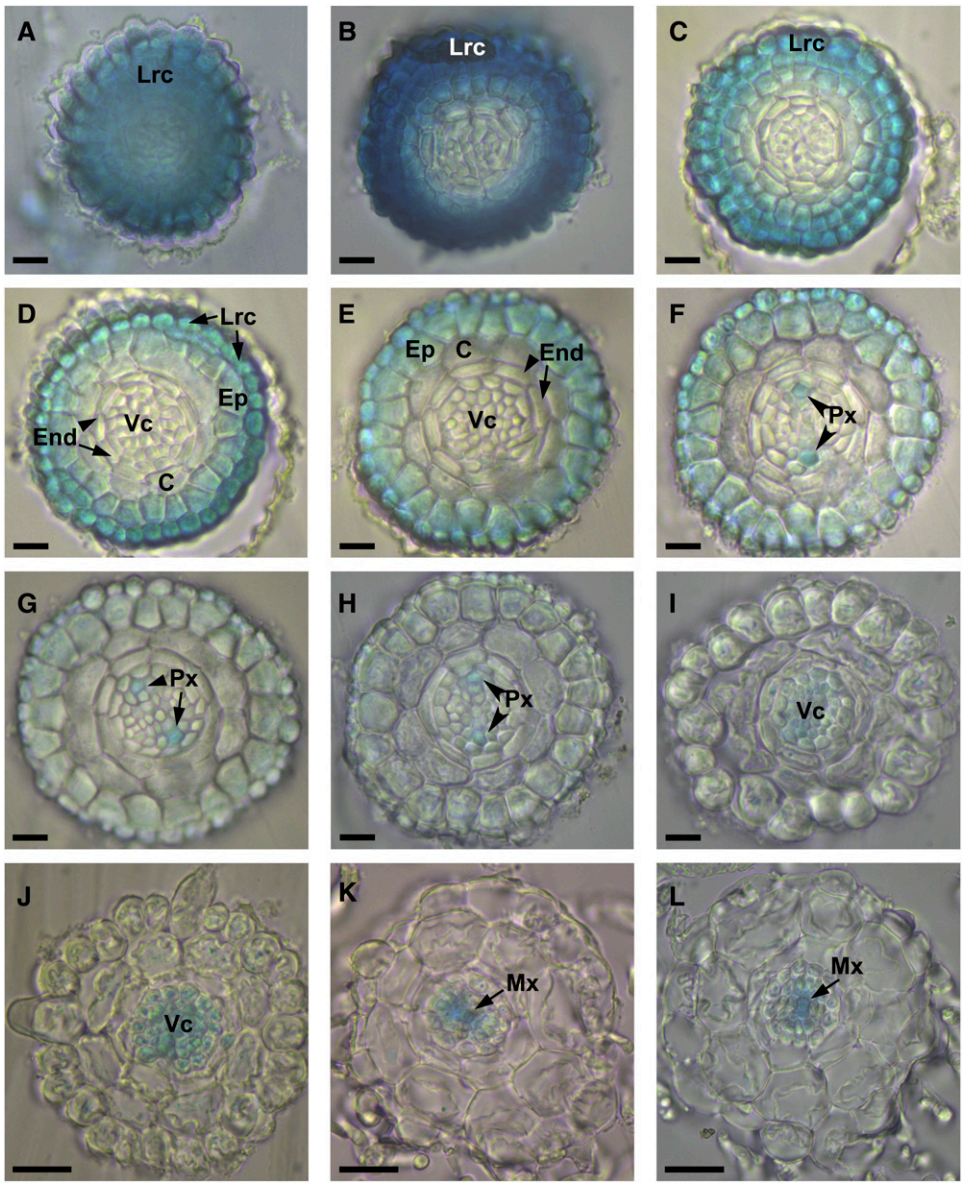

Figure 2. *AtAO1* tissue expression pattern in cross sections of primary roots from 4-d-old seedlings. Light microscopy analysis of root cross sections is shown after GUS staining of *AtAO1*::*GFP-GUS* transgenic plants. Highly reproducible results were obtained from three independent transgenic lines. The staining reaction was allowed to proceed overnight. C, Cortex; End, endodermis; Ep, epidermis; Lrc, lateral root cap; Mx, metaxylem; Px, protoxylem; Vc, vascular cylinder. A to E, Meristematic zone. F, Transition zone. G and H, Elongation zone. I to L, Maturation zone. Micrographs are representative of those obtained from three independent experiments. Bars = 25 μm (A–I) and 50 μm (J–L).

TAIR accession no. 4284859) were identified from the TAIR database (http://www.arabidopsis.org/; Swarbreck et al., 2008) and hereafter are referred as *Atao1.1* and *Atao1.2* mutants. From evidence available in TAIR, the T-DNA insertion site is located in the third exon in *Atao1.1*, between the nucleotide triplets encoding two putative copper-binding His residues important for enzyme catalytic activity (Møller et al., 1998), and in the first exon in *Atao1.2* (Supplemental Figs. S1 and S2), creating loss-of-function mutants. Mutant plants homozygous for the T-DNA insertions were selected by PCR analysis of genomic DNA (Supplemental Fig. S1). Reverse transcription (RT)-PCR analysis of the selected plants confirmed the absence of the full-length gene transcripts in *Atao1.1* and *Atao1.2* mutants (Supplemental Fig. S1). The presence of a single-locus T-DNA insertion has been confirmed by Southern-blot analysis in the *Atao1.1* mutant (Supplemental Fig. S1). Analysis of the *Atao1* mutants under physiological growth conditions did not reveal any apparent defective phenotype, such as stem and root length, leaf morphology, inflorescence characteristics (data not shown), or the length of root meristematic zone (approximately 210 μm in the wild type, *Atao1.1*, and *Atao1.2*).

Taking into account the previously suggested involvement of MeJA in xylogenesis (Fattorini et al., 2009) along with the proposed participation of AtAO1 or ZmPAO in root vascular differentiation, respectively, upon nematode invasion (Møller et al., 1998) or under stress-like conditions (Tisi et al., 2011a, 2011b), LSCM analysis was carried out to visualize xylem tissue alteration following MeJA treatment in the wild type and *Atao1* mutants. In particular, we focused our attention on protoxylem differentiation timing, considering as a

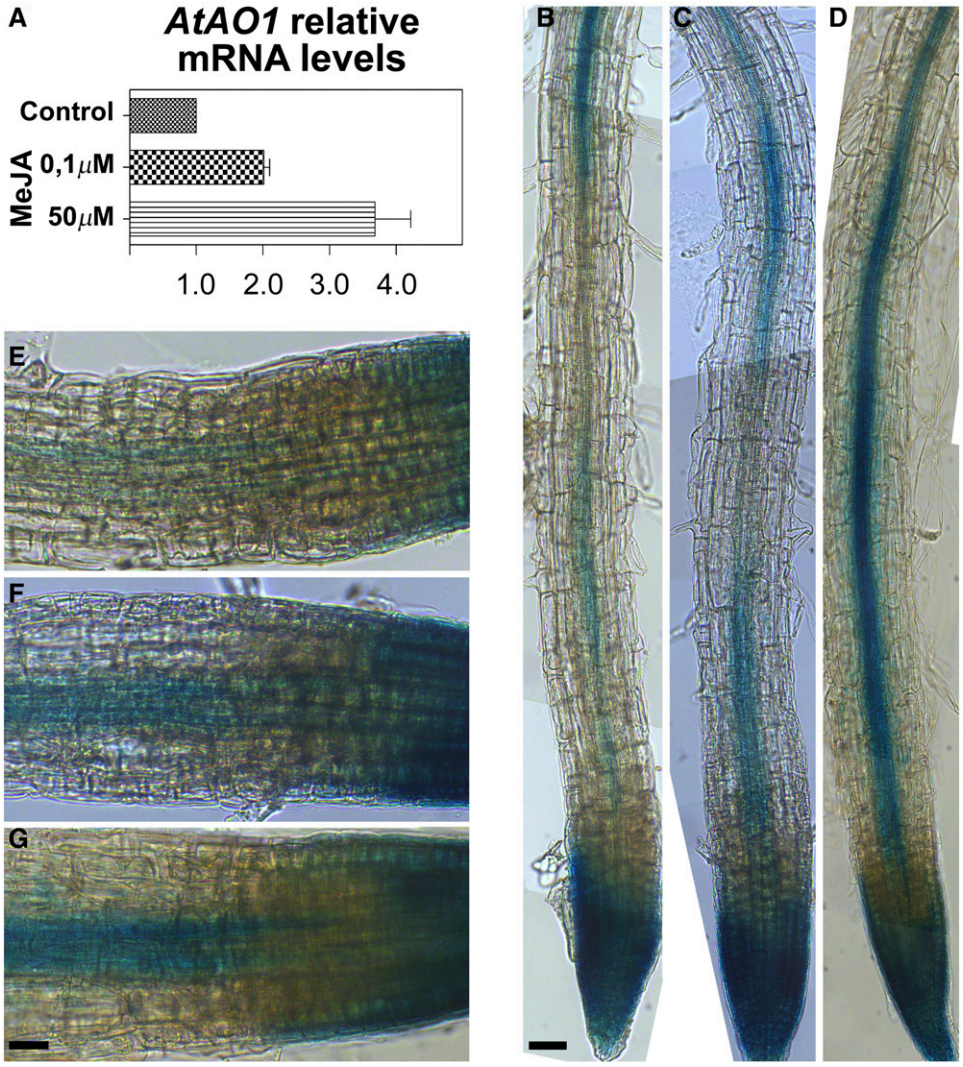

Figure 3. Analysis of *AtAO1* gene expression upon MeJA treatment by RT-qPCR and GUS staining analysis. A, Expression of the *AtAO1* gene was analyzed in 7-d-old wild-type seedlings untreated (Control) or treated with 0.1 or 50 μM MeJA for 1 h. Two biological replicates, each with three technical replicates, were performed. Relative *AtAO1* mRNA levels are reported (means ± SD; $n = 2$). B to G, Light microscopy analysis after GUS staining of roots of 4-d-old *AtAO1*::*GFP-GUS* transgenic plants untreated (B and E) or treated with 0.1 μM MeJA (C and F) or 50 μM MeJA (D and G) for 1 h. The staining reaction was allowed to proceed for 1 h after hormone treatment. Micrographs are representative of those obtained from 25 roots from five independent experiments. Bars = 50 μm (B–D) and 25 μm (E–G).

reference event the final step of the secondary cell wall-thickening process. Figure 4 shows the appearance of protoxylem cells at the final step of secondary cell wall differentiation, simultaneously investigated by both bright-field microscopy and LSCM. In this regard, as revealed in Figure 4C, the boundary between cells with and without fully developed secondary cell wall thickenings visible in bright-field images (Fig. 4A; Supplemental Fig. S3) coincides with the PI fluorescence transition point observed by LSCM analysis (Fig. 4B). Figure 5A shows that, in the absence of treatment, roots of both *Atao1* mutants present no apparent altered phenotype in xylem tissues in comparison with wild-type roots (Supplemental Figs. S3 and S4). Indeed, the first protoxylem cells with fully developed secondary cell wall thickenings appeared at approximately 1,080, 1,050, and 1,020 μm from the apical meristem, respectively, in roots of untreated wild-type, *Atao1.1*, and *Atao1.2* control plants (Fig. 5A; Supplemental Figs. S3 and S4). Interestingly, 50 μM MeJA treatment induced early protoxylem differentiation in roots of wild-type plants (first cells with fully developed secondary cell wall thickenings at approximately 540 μm from the apical meristem), without affecting protoxylem differentiation in *Atao1* mutants (first cells with fully developed secondary cell wall thickenings at approximately 950 and 975 μm from the apical meristem in *Atao1.1* and *Atao1.2* mutants, respectively; Fig. 5A; Supplemental Fig. S5). On the other hand, the meristem size, which is defined by the transition between cell proliferation and cell differentiation, was similarly reduced in the wild type and *Atao1* mutants upon 50 μM MeJA treatment (length of root meristematic zone, approximately 110 μm) as compared with untreated samples (length of root meristematic zone, approximately 210 μm).

Lowering MeJA concentrations to 0.1 μM still resulted in selective induction of early protoxylem differentiation in wild-type plants (approximately 560 μm from the apical meristem; Fig. 5A; Supplemental Fig. S5), without any effect in the two *Atao1* mutants (Fig. 5A; Supplemental Fig. S5). In this condition, the length of the meristematic zone appeared reduced in wild-type plants

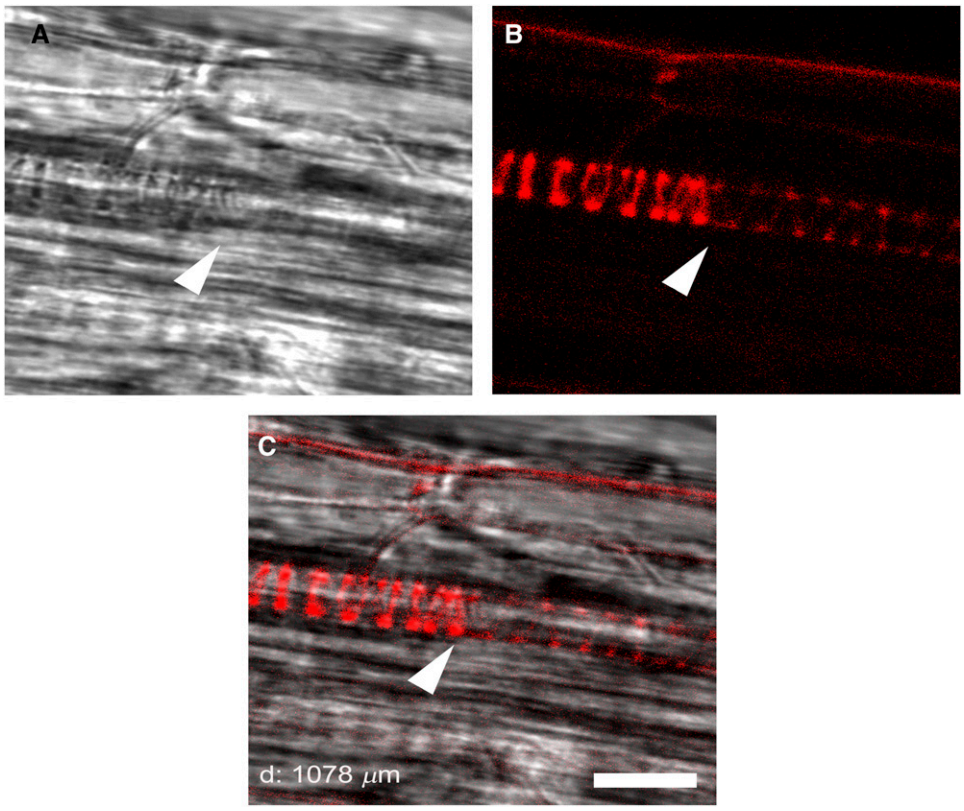

Figure 4. Confocal microscopic analysis of the site of appearance of the first protoxylem cells with fully developed secondary wall thickenings in root apices of 14-d-old wild-type Arabidopsis seedlings. Arrowheads indicate the site of appearance of the first protoxylem cells with fully developed secondary wall thickenings used in measurements of xylem distance. A, Bright-field image showing the boundary between cells with and without fully developed secondary cell wall thickenings. B, The respective LSCM analysis after PI staining showing the sharp intensification of fluorescence at the site of appearance of protoxylem cells with fully developed secondary cell wall thickenings. C, PI and bright-field overlay image. Bar = 10 μm.

(approximately 125 μm from the quiescent center), while its value remained unchanged in both *Atao1* mutants (approximately 210 μm from the quiescent center). Interestingly, in the JA-insensitive Arabidopsis mutant of CORONATINE-INSENSITIVE PROTEIN1, *Atcoi1-16*, grown under physiological conditions, no alterations in *AtAO1* gene expression or in root protoxylem differentiation were observed (data not shown).

Moreover, the effect of MeJA supply on the root growth of wild-type and both *Atao1* mutant plants was examined. As shown in Figure 5B, treatment with MeJA at different concentrations (ranging from 0.1 to 50 μM) similarly inhibited root growth in the wild type and both *Atao1* mutants, depending on the hormone concentration.

CuAO activity has been showed to be induced by abscisic acid (ABA) in the cell wall of rice (*Oryza sativa*) roots (Lin and Kao, 2001), and ABA biosynthesis has been linked to drought-induced MeJA accumulation in rice panicles (Kim et al., 2009). To explore if MeJA induction of the *AtAO1*-mediated early protoxylem differentiation occurs via ABA signaling, the effect of ABA on root growth and xylem differentiation in wild-type and *Atao1* plants was also analyzed. The results showed that ABA similarly affects root phenotype in these plants at both tested concentrations (0.1 and 1 μM), inducing early protoxylem differentiation to the same extent in each analyzed genotype, without affecting root growth (Supplemental Fig. S6). Consistently, and in agreement with the previously cited microarray data available in the Arabidopsis eFP Browser, RT-qPCR analysis showed that *AtAO1* expression is not induced by ABA treatment in 7-d-old whole seedlings (Supplemental Fig. S6).

To examine whether AtAO1 activity mediates auxin and/or cytokinin signaling involved in root growth and xylem differentiation, the effect of 1-naphthaleneacetic acid (NAA) or 6-benzylaminopurine (BA) treatment on these events was investigated in roots of wild-type and mutant plants. Both exogenous BA and NAA affected root growth and xylem differentiation (Supplemental Fig. S6) in roots of the wild type and *Atao1* mutants in a similar manner. In particular, in all the analyzed genotypes, NAA was ineffective in altering the pattern of protoxylem differentiation (Supplemental Fig. S6), while BA strongly delayed this event (Supplemental Fig. S6). Consistently, RT-qPCR analysis showed that neither BA nor NAA treatment altered *AtAO1* expression (Supplemental Fig. S6).

AtAO1-Driven Production of H_2O_2 Signals the Induction of Root Protoxylem Differentiation upon MeJA Treatment

To investigate the possible role of AtAO1-produced H_2O_2 in MeJA-induced xylem differentiation, wild-type and *Atao1* plants were simultaneously treated with 0.1 μM MeJA and the H_2O_2 scavenger DMTU at the working concentration of 100 μM, as reported previously in roots of onion (*Allium cepa*; Murali Achary and Panda, 2010). The results showed that DMTU reversed both the

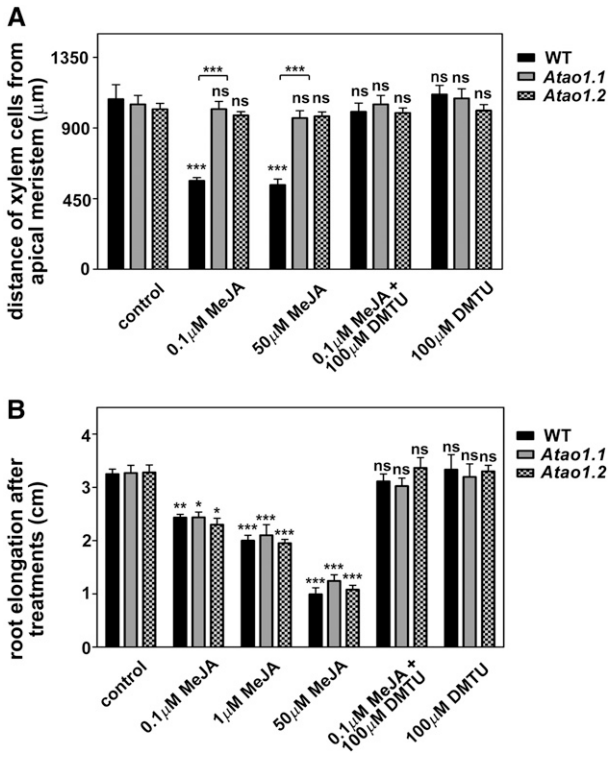

Figure 5. Effect of MeJA and/or *N,N*[1]-dimethylthiourea (DMTU) treatments on protoxylem differentiation and root growth in the wild type (WT) and *Atao1* mutants. Analyses were carried out on 14-d-old seedlings treated with MeJA and/or DMTU for the last 7 d. A, Distance from the apical meristem of the first protoxylem cells with fully developed secondary cell wall thickenings (means ± SD; $n = 25$). B, Increase in root length representing the difference between root length measured after 7 d of treatment and that measured at the onset of the treatment (means ± SD; $n = 25$). Control indicates untreated plants. The significance levels between the treated plants and the corresponding untreated control plants are reported for each treatment, while the significance levels between the wild type and *Atao1* mutants supplied with the same concentration of chemicals (horizontal square brackets) are reported only when $P \leq 0.05$. ns, Not significant, $P > 0.05$; *, $P \leq 0.05$; **, $P \leq 0.01$; ***, $P \leq 0.001$.

MeJA-induced early protoxylem differentiation and the early transition from the division to the elongation zone in wild-type plants, while having no effect in MeJA-treated *Atao1* mutants. In fact, in wild-type plants, the distance from the apical meristem of cells with fully developed secondary cell wall thickenings and meristem size recovered to approximately 1,000 μm (Fig. 5A; Supplemental Fig. S5) and approximately 190 μm, respectively, upon DMTU treatment. Moreover, DMTU treatment was effective in reversing 0.1 μM MeJA-induced inhibition of root length in the wild type and both *Atao1* mutants (Fig. 5B). Treatment with DMTU alone affected neither protoxylem differentiation (Fig. 5A) nor root length (Fig. 5B).

Successively, we have verified whether MeJA treatment resulted in detectable changes of H_2O_2 levels in differentiating xylem tissues. Figure 6 shows the in situ visualization by LSCM of H_2O_2 accumulation using an Amplex Ultra Red (AUR)-specific assay in roots of the wild type and both *Atao1* mutants treated or not with 0.1 μM MeJA for 7 d (Fig. 6, A and B; Supplemental Fig. S7). In roots of untreated wild-type plants and untreated and MeJA-treated *Atao1* mutants, H_2O_2-dependent AUR fluorescence was not detectable at the site of differentiating protoxylem elements (approximately 1,080, 1,050, 1,020, 1,030, and 980 μm; Supplemental Fig. S7). On the other hand, in MeJA-treated wild-type roots, a clearly detectable H_2O_2-dependent AUR fluorescence was revealed in the root zone where the first protoxylem cells with fully developed secondary cell wall thickenings are found (approximately 560 μm; Fig. 6A), visible both in protoxylem cell walls and external medium. The above-reported results confirmed that AtAO1 activity is the source of H_2O_2 influencing protoxylem differentiation upon MeJA treatment. The intense staining of the external medium is likely due to the release of H_2O_2 from the tissues corresponding to a higher production of this ROS through an increased AtAO1 activity.

MeJA Treatment Negatively Affects Put Levels in Wild-Type Roots

We analyzed whether MeJA treatment resulted in altered PA levels by controlling the amount of free soluble PAs in roots from the wild type and both *Atao1* mutants, untreated or treated with 0.1 or 50 μM MeJA (Fig. 6, C and D; Supplemental Fig. S8). Interestingly, MeJA treatment induced a dose-dependent depletion of the preferred AtAO1 substrate Put in wild-type roots without affecting Put levels in roots of both *Atao1* mutants, confirming that AtAO1 is involved in the MeJA-induced oxidative catabolism of Put in Arabidopsis roots. In detail, Put levels were 34% and 46% lower, respectively, in 0.1 and 50 μM MeJA-treated wild-type roots as compared with the values measured in untreated wild-type roots after 4 d of treatment, recovering control levels after 6 d (Fig. 6, C and D). Consistently, in roots of both *Atao1* mutants, MeJA treatment did not induce a significant variation in Put levels as compared with the corresponding untreated roots at any analyzed times from the onset of the treatment (Fig. 6, C and D).

MeJA treatments (0.1 and 50 μM) did not significantly affect Spd levels in roots of the wild type or *Atao1* mutants (Supplemental Fig. S8), while at the highest tested concentration, a similar increase of Spm levels in wild-type and mutant plants was observed (Supplemental Fig. S8).

Exogenously Supplied Put Affects Root Growth and Protoxylem Differentiation via AtAO1-Mediated H_2O_2 Production

In order to obtain further evidence of the involvement of AtAO1 activity in xylem differentiation, the AtAO1 substrate Put (Møller et al., 1998) was provided at three different concentrations to wild-type, *Atao1.1*, and *Atao1.2* plants. Figure 7 shows the results obtained.

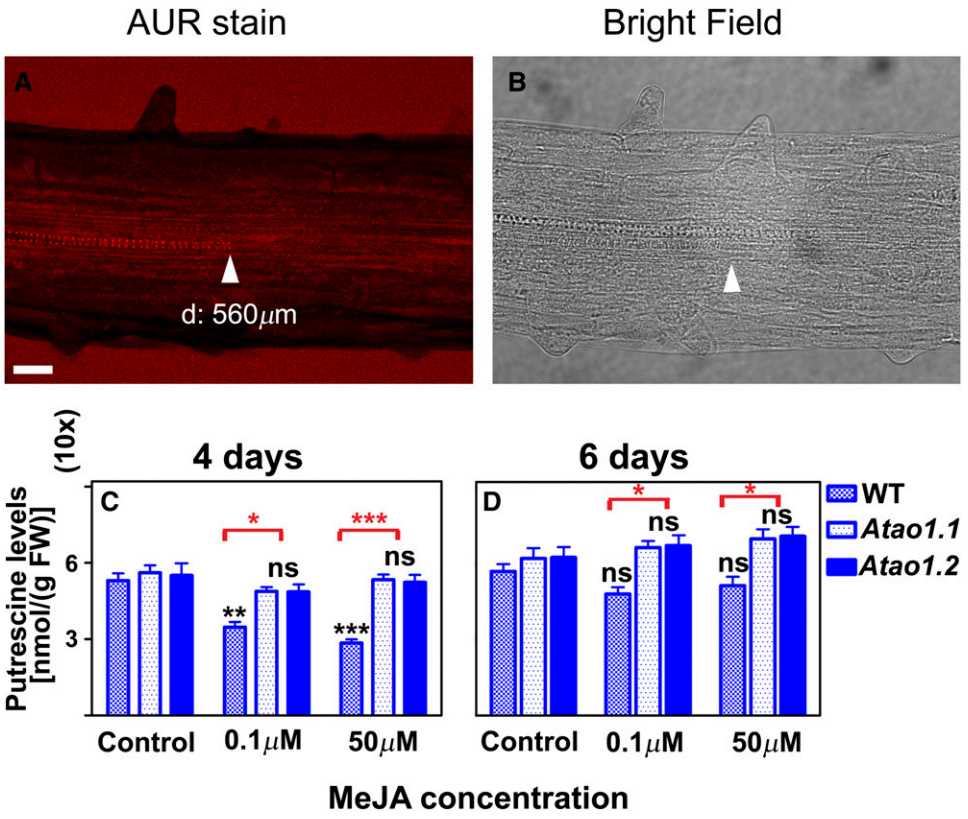

Figure 6. Effect of MeJA treatment on H_2O_2 accumulation and free soluble Put levels in roots of the wild type (WT) and *Atao1* mutants. A and B, In situ H_2O_2 detection by LSCM analysis after AUR staining (A) and corresponding bright-field image (B) of roots from 14-d-old wild-type seedlings after treatment with 0.1 μM MeJA for the last 7 d. Images show the root zone where the first protoxylem cells with fully developed secondary wall thickenings are found. Micrographs are relative to the central section of the root. d, Average distance from the apical meristem of the first protoxylem cells with secondary cell wall thickenings. Micrographs are representative of those obtained from 25 roots from five independent experiments. Bar = 40 μm. C and D, Free soluble Put levels expressed on a fresh weight (FW) basis in roots of the wild type and *Atao1* mutants upon 0.1 or 50 μM MeJA treatment (means ± SD; $n = 5$). Analyses were carried out on 11-d-old seedlings untreated or treated with MeJA for 4 d (C) or 13-d-old seedlings untreated or treated with MeJA for 6 d (D). Control indicates untreated plants. The significance levels between MeJA-treated plants and the corresponding control plants are reported in black, while the significance levels between the wild type and *Atao1* mutants supplied with the same concentration of MeJA are reported only when $P \leq 0.05$ in red. ns, Not significant, $P > 0.05$; *, $P \leq 0.05$; **, $P \leq 0.01$; ***, $P \leq 0.001$.

Treatment with Put at either 10 μM (Fig. 7A; Supplemental Figs. S9 and S10) or 100 μM (Fig. 7A) induced early protoxylem differentiation in wild-type plants (first cells with fully developed secondary cell wall thickenings at approximately 720 μm from the apical meristem) but not in *Atao1* mutants as compared with the corresponding untreated plants. Conversely, a lower Put concentration (1 μM) was ineffective (Fig. 7A). Remarkably, root growth was not affected by Put treatment at the tested concentrations (Fig. 7B) in the wild type and the *Atao1* mutants. Treatment with 10 μM Spd induced early protoxylem differentiation to the same extent in the wild type and both *Atao1* mutants (first cells with fully developed secondary cell wall thickenings at approximately 750 μm from the apical meristem; data not shown).

Moreover, with the aim to corroborate the hypothesis that the effect of exogenously supplied Put on protoxylem differentiation in wild-type plants is mediated by the H_2O_2 produced via AtAO1-driven oxidation, plant treatment with DMTU was exploited. In plants treated with 10 μM Put and 100 μM DMTU, the latter reversed the Put-induced effect on protoxylem differentiation. Indeed, the first cells with fully developed secondary cell wall thickenings appeared at approximately 950 μm, while no effect in the roots of both *Atao1* mutants was observable (Fig. 7A; Supplemental Fig. S9).

AtAO1-Overexpressing Plants Show Early Protoxylem Differentiation

We further investigated the role played by AtAO1 in root xylem tissue differentiation through the analysis of transgenic Arabidopsis plants overexpressing *AtAO1* (over*AtAO1*). Figure 8 shows the phenotype characterization of over*AtAO1* lines. Among the various independent lines selected by RT-PCR and western-blot analysis,

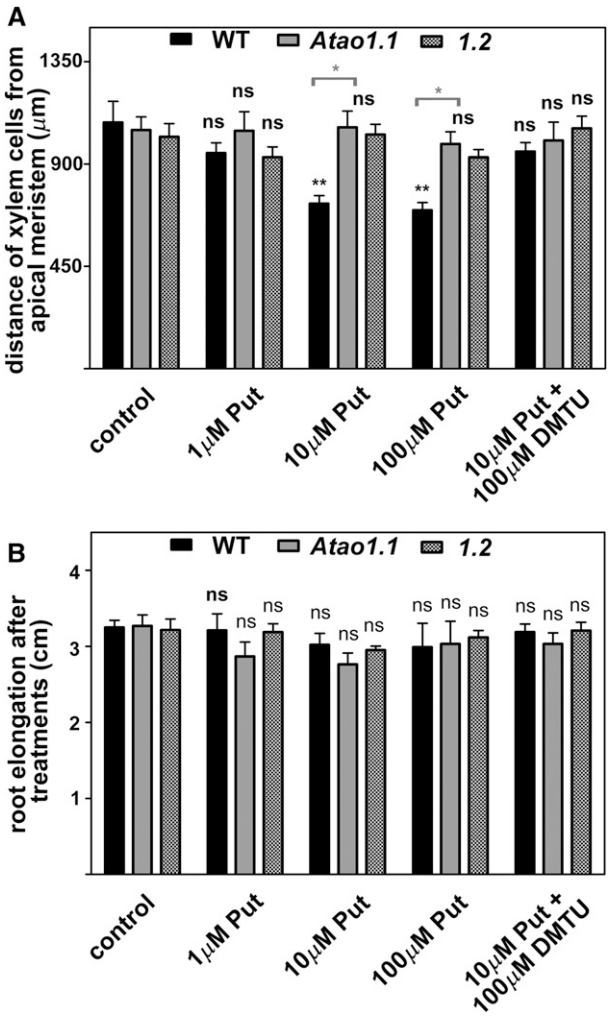

Figure 7. Effects of exogenously supplied Put and/or DMTU on both protoxylem differentiation and root growth in the wild type (WT) and *Atao1* mutants. Analyses were carried out on 14-d-old seedlings treated with 1, 10, or 100 μM Put or 10 μM Put and 100 μM DMTU for the last 7 d. A, Distance from the apical meristem of the first protoxylem cells with fully developed secondary cell wall thickenings measured after 7 d of treatment (means ± SD; $n = 25$). B, Increase in root length representing the difference between root length measured after 7 d of treatment and that measured at the onset of the treatment (means ± SD; $n = 25$). The significance levels between the treated plants and the corresponding untreated plants are reported for each treatment, while the significance levels between the wild type and *Atao1* mutants supplied with the same concentration of chemicals (horizontal square brackets) are reported only when $P \leq 0.05$. Control indicates untreated plants. ns, Not significant, $P > 0.05$; *, $P \leq 0.05$; **, $P \leq 0.01$; ***, $P \leq 0.001$.

lines 16, 11, and 3 showed progressively higher expression levels of the transgene and were chosen for further analysis (Fig. 8D). These transgenic lines showed a significant reduction in Put levels as compared with wild-type plants, and the extent of the decrease (line 3, 55%; line 11, 57%; line 16, 16%) correlated with AtAO1 expression levels (Fig. 8C). Similarly, Spd and Spm levels were lower in both line 3 (showing decreases of 26% for Spd and 24% for Spm) and line 11 (showing decreases of 25% for Spd and 21% for Spm) than in the wild type, while being unaltered in line 16 (Supplemental Fig. S11). Investigation of the root phenotype in 18-d-old transformed plants of lines with the highest expression levels (lines 3 and 11) revealed the occurrence of a slight root growth inhibition (Fig. 8A) and early protoxylem differentiation (first protoxylem cells with fully developed secondary cell wall thickenings at approximately 630 and 570 μm, respectively, from the apical meristem; Fig. 8B; Supplemental Fig. S12). This was not the case in line 16, which presented the lowest ATAO1 protein level (Fig. 8, B and D; Supplemental Fig. S12). In all cases, a reduction in the length of the meristematic zone was observed, which was consistent with the high levels of recombinant AtAO1 protein (approximately 125, 140, and 170 μm from the quiescent center in lines 11, 3, and 16, respectively). Moreover, as shown in Figure 9, at the site where the first protoxylem cells with fully developed secondary wall thickenings are found, relevant H_2O_2 levels in external medium and protoxylem have been revealed by AUR fluorescence assay in both transgenic lines 11 (Fig. 9A) and 3 (Fig. 9, B–D) but not in transgenic line 16 (Supplemental Fig. S13) and wild-type plants (data not shown), similar to what was observed in 14-d-old wild-type plants (Supplemental Fig. S7).

DISCUSSION

MeJA Induces *AtAO1* Gene Expression in Developing Protoxylem Tissues in the Root Apex

The analysis of the *AtAO1* expression pattern in primary roots carried out by exploiting a promoter::*GFP-GUS* fusion revealed vascular tissue localization, in particular in the root apical region. Signal was visible in the transition, elongation, and maturation zones as well as the in root cap cells (Figs. 1 and 2). In this respect, previous results suggested that ROS released through PA catabolism behave as signals for secondary wall deposition and/or for the induction of developmental PCD in differentiating xylem elements and sloughed root cap cells (Tisi et al., 2011b). Thus, *AtAO1* expression in root protoxylem tissues, especially at the site of the final step of secondary cell wall thickening (Fig. 1), strongly suggests its involvement in the final stages of protoxylem cell differentiation, in particular those concerning cell wall maturation that necessarily precede terminal cell death.

Moreover, considering that *AOs* are well-known JA-inducible genes (Cona et al., 2006; Angelini et al., 2008) and that *AtAO1* gene expression has been shown to increase in the root vascular tissues as a consequence of nematode infection (Møller et al., 1998), we analyzed the effect of MeJA treatment on *AtAO1* tissue-specific expression in the root. Data obtained by RT-qPCR analysis showed that *AtAO1* expression was induced by MeJA treatments, even at very low concentrations (Fig. 3). In

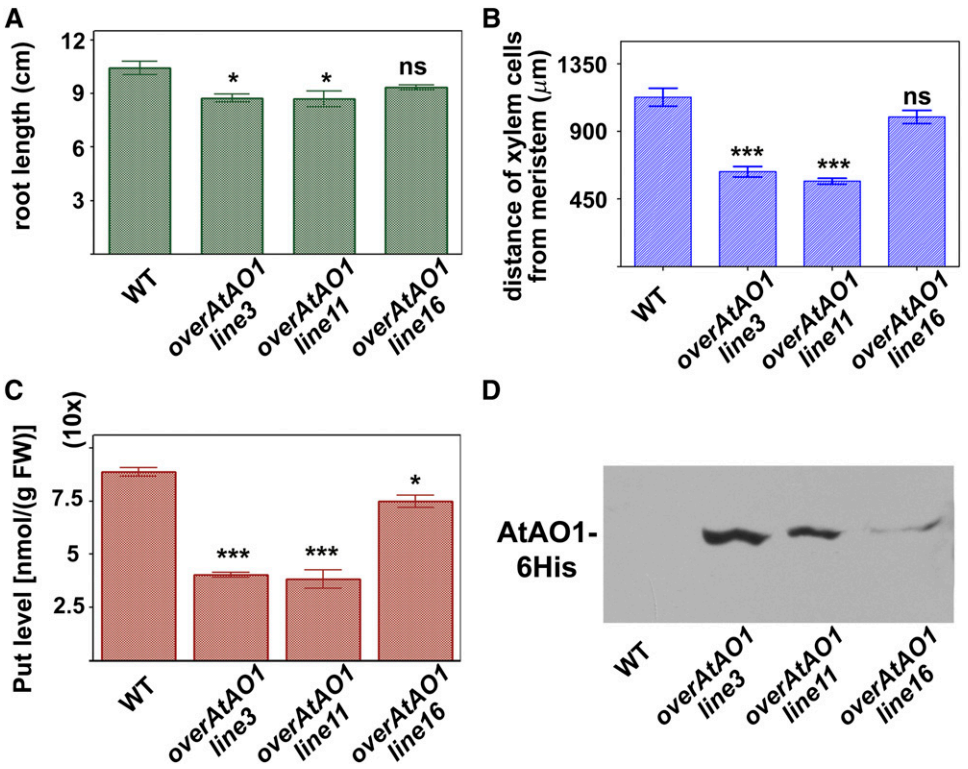

Figure 8. Effects of AtAO1 overexpression on root growth, protoxylem differentiation, and Put levels. A and B, Root length (A) and distance from the apical meristem of the first protoxylem cells with fully developed secondary wall thickenings (B) measured in 18-d-old wild-type (WT) and over*AtAO1* seedlings (means ± SD; $n = 25$). C, Free soluble Put levels expressed on a fresh weight (FW) basis in roots of 18-d-old wild-type and over*AtAO1* Arabidopsis seedlings (means ± SD; $n = 5$). ns, Not significant, $P > 0.05$; *, $P \leq 0.05$; ***, $P \leq 0.001$. D, Western-blot analysis of crude extract from wild-type and over*AtAO1* plants using an anti-His tag antibody after SDS-PAGE loaded on the basis of total protein content.

particular, analysis of the AtAO1 tissue-specific expression in roots of MeJA-treated plants showed that the intensity of GUS staining was enhanced in the vascular tissues of the elongation and division/differentiation transition zones (Fig. 3). Interestingly, an earlier developmental expression pattern occurred after MeJA treatment, as shown by the appearance of GUS staining in a location closest to the root tip, suggesting a role of AtAO1 in MeJA signaling leading to protoxylem differentiation.

H_2O_2 from AtAO1-Driven Put Oxidation Signals the MeJA-Induced Protoxylem Differentiation

In a few recent reports, a still quite unexplored role for MeJA in xylem development was suggested (Cenzano et al., 2003; Fattorini et al., 2009). In this regard, exogenous JA and MeJA have been shown to induce early xylem differentiation in potato stolons (Cenzano et al., 2003) and xylogenesis in tobacco thin cell layers (Fattorini et al., 2009), respectively. This work reveals that MeJA treatment results in early protoxylem differentiation in Arabidopsis wild-type seedlings (Fig. 5; Supplemental Figs. S3 and S5), without affecting it in *Atao1* mutants (Fig. 5; Supplemental Figs. S4, S5, and S10), hence suggesting the involvement of AtAO1 in the MeJA-induced differentiation of root vascular tissues. Notably, MeJA, unlike the dose-dependent effect exerted on root growth, was equally effective in inducing protoxylem differentiation in wild-type seedlings at both 0.1 and 50 μM (Fig. 5; Supplemental Figs. S3 and S5). Moreover, the occurrence of a similar root growth rate (Fig. 5) but dissimilar protoxylem differentiation timing (Fig. 5; Supplemental Figs. S3–S5 and S10) in the wild type and *Atao1* mutants upon MeJA treatment revealed the potential specificity of *AtAO1*'s role in the MeJA-induced vascular differentiation, independently of the inhibitory effect on root growth. Furthermore, the total ineffectiveness of the same treatment in altering protoxylem differentiation in *Atao1* mutants showed the likely absence of any concurrent MeJA signaling pathway unconnected to AtAO1-mediated PA catabolism.

The analysis of free PA levels showed that Put was selectively reduced upon MeJA supply in wild-type roots without undergoing any significant change in equally treated mutant roots (Fig. 6). On the other hand, Spd levels remained unchanged in both wild-type and mutant plants, while Spm levels were similarly affected. This may exclude the involvement of Spd and Spm catabolism in the observed MeJA-induced phenotype (Supplemental Fig. S8). These data, together with the reversion effect exerted by DMTU on 0.1 μM MeJA-induced early protoxylem differentiation in wild-type roots (Fig. 5; Supplemental Figs. S3 and S5) and the increased accumulation of H_2O_2 upon the same treatment at the site of appearance of protoxylem cells with fully developed secondary wall thickenings (Fig. 6; Supplemental Fig. S7), support the hypothesis that MeJA's effect on protoxylem differentiation could be mediated by the H_2O_2 produced via AtAO1-driven Put oxidation. This possibility is consistent with the previously suggested hypothesis in which both apoplastic AO

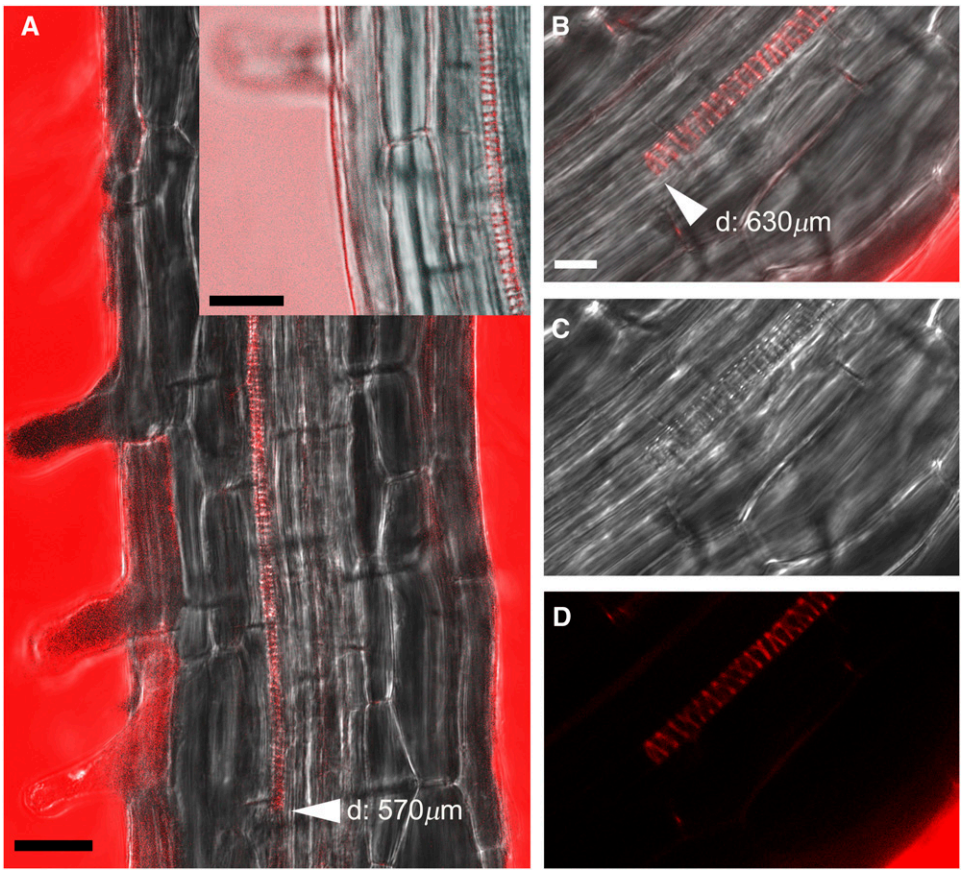

Figure 9. In situ H_2O_2 detection by AUR staining in roots of 18-d-old over*AtAO1* seedlings. Images show the root zone where the first protoxylem cells with fully developed secondary cell wall thickenings are found. A, AUR and bright-field overlay images of roots from over-*AtAO1* line 11 after incubation for 10 or 5 min (inset) in staining solutions. The inset shows a detail of the zone at a later developmental stage with respect to the starting site of H_2O_2 production. B to D, AUR and bright-field overlay image (B), bright-field image (C), and AUR staining (D) of roots from over-*AtAO1* line 3 after incubation for 10 min in staining solution. d, Average distance from the apical meristem of the first protoxylem cells with secondary cell wall thickenings. Bars = 25 μm (A and inset) and 10 μm (B).

levels and PA secretion in the cell wall increase under stress growth conditions, with a consequent decrease of the PA-H_2O_2 ratio and the activation of defense responses (Moschou et al., 2008; Tisi et al., 2011a). Consistently, the unresponsiveness of the *Atao1* mutants to MeJA treatment demonstrated the involvement of *AtAO1* in root xylem differentiation in response to a hormone that is well known to play a role in defense response signaling. Interestingly, treatment with DMTU alone did not affect xylem differentiation in the wild type and *Atao1* mutants (Fig. 5). This result, along with the absence of an observable defective phenotype in *Atao1.1* and *Atao1.2* seedlings under physiological growth conditions, encouraged us to hypothesize the involvement of AtAO1 in xylem differentiation under stress growth conditions, such as those signaled by MeJA. Moreover, the absence of an alteration in protoxylem phenotype or *AtAO1* gene expression in the *Atcoi1-16* mutant grown under physiological conditions further supported the above-mentioned hypothesis, suggesting that the absence of JA signaling becomes crucial only under stress conditions when an early protoxylem differentiation is observed.

AtAO1 Is Not Involved in ABA, BA, or NAA Signaling

It has been reported recently that the addition of PAs and ABA resulted in an increase of H_2O_2 levels in Arabidopsis primary roots and that a mutant for another CuAO-encoding gene (At1g62818), namely *cuao1*, was less sensitive to ABA-induced root growth inhibition as compared with the wild type (Wimalasekera et al., 2011). Since the existence of signal cross talk between MeJA and ABA has been suggested to occur in guard cells (Munemasa et al., 2011) and in rice panicles (Kim et al., 2009) during drought conditions, the effect of ABA treatment on root growth and xylem differentiation of the wild type and *Atao1* mutants was analyzed. Unlike MeJA, ABA similarly affected root development in the wild type and both *Atao1* mutants, inducing early protoxylem differentiation to the same extent in both wild-type and mutant plants without affecting root growth (Supplemental Fig. S6). Hence, the absence of any evident difference in phenotype between *Atao1* and wild-type roots upon ABA treatment, along with the unchanged *AtAO1* gene expression levels in the hormone-treated wild-type plants, present us with two possibilities: either *AtAO1* is not involved in ABA signaling or it participates upstream in JA signaling leading to the induction of ABA biosynthesis. The latter hypothesis is suggested by the previously observed effect of the drought-induced MeJA accumulation on the ABA biosynthetic pathway (Kim et al., 2009).

As the role of auxin and cytokinin in vascular patterning has been extensively reported (Bishopp et al., 2011), here we analyzed the effect of NAA and BA supply on root growth and xylem differentiation of

wild-type and *Atao1* plants. The analysis of the root phenotype upon BA and NAA exogenous supply showed that the wild type and *Atao1* mutants were similarly affected by each hormone. Indeed, in the three genotypes, while both hormones exerted similar inhibitory effects on root growth, BA treatment delayed protoxylem differentiation, which was unaffected by NAA (Supplemental Fig. S6). In this regard, analysis of cytokinin response mutants and the effect of exogenously supplied cytokinin have shown that this hormone inhibits protoxylem differentiation (Mähönen et al., 2006). Furthermore, the inefficiency of NAA treatment in altering xylem differentiation is not surprising, considering that it has been reported previously that exogenous auxin has no effect on vascular patterning (Cui et al., 2011). Overall, the analysis of the root phenotype of the wild type and *Atao1* mutants along with the unresponsiveness of *AtAO1* gene expression following ABA, BA, or NAA treatment suggest that *AtAO1* is not involved in the corresponding signaling pathways leading to the alteration of root growth and/or xylem differentiation.

On the other hand, our results may indicate AtAO1 as one of the systems responsible for H_2O_2 accumulation that is required for differentiation in the context of the control of the transition between cell proliferation and differentiation in the root meristem independent of the cytokinin/auxin antagonistic interaction (Tsukagoshi et al., 2010).

MeJA-Induced AtAO1 Influences Protoxylem Position Independently of Total Root Elongation and Meristem Size

Root meristem size is defined by the transition between cell proliferation and cell differentiation. Two independent systems have been implicated in the control of the cell division/differentiation balance regulating meristem size in the Arabidopsis root: the antagonist auxin/cytokinin network (Petricka et al., 2012) and the redox regulation (Tsukagoshi et al., 2010), cell division being promoted by auxin or superoxide anion and cell differentiation being induced by cytokinin or H_2O_2.

Root length, meristem height, and its relative distance to the most proximal protoxylem tracheary element have been reported to be spatially correlated in pea (*Pisum sativum*) seedlings through a growth rate-dependent relationship (Rost and Baum, 1988). However, this correlation has been found to cease if a perturbation of cell division and/or cell elongation occurs by stress treatments or hormone action (Rost and Baum, 1988). Consistently, our results show that in hormone-treated plants, root elongation and protoxylem distance from the apical meristem are unrelated. Indeed, (1) treatment with 0.1 μM ABA did not affect root length, while moving the protoxylem position toward the root tip; (2) 0.1 μM BA, consistent with what was reported by Mähönen et al. (2006), inhibited root elongation but strongly delayed protoxylem differentiation; (3) 0.1 μM NAA reduced root growth without exerting any modulation on protoxylem position (Supplemental Fig. S6); and (4) MeJA induced protoxylem differentiation at both concentrations used independently of the strength of their effect on root elongation (Fig. 5; Supplemental Figs. S3–S5 and S10).

It has been reported that JA-induced inhibition of root elongation is a complex process occurring by the reduction of both cell number and cell length in the elongation and differentiation zones as well as through the inhibition of cell division activity in meristem cells that results in smaller meristem size (Chen et al., 2011). JA, supplied at the concentration of 20 μM, has been shown to interfere with the auxin pathway by repressing the auxin-induced transcription factors PLETHORA1 (PLT1) and PLT2 (Chen et al., 2011), which influence stem cell niche maintenance and meristem activity as well as the size and location of root developmental zones (Mähönen et al., 2014). The fact that 0.1 μM MeJA altered meristem dimensions in wild-type seedlings, the effect being DMTU reversible, but not in *Atao1* mutants suggests that, under our experimental conditions, the meristem dimensions are dependent on AtAO1 activity, in agreement with the hypothesis reported by Tsukagoshi et al. (2010) that division/differentiation transition zone position and meristem size may depend on ROS distribution. Thus, the early protoxylem differentiation observed in wild-type roots treated with 0.1 μM MeJA could be considered a consequence of the smaller meristem and/or a specific effect of MeJA. Nevertheless, since MeJA at higher concentration decreases meristem size in both the wild type and *Atao1* without altering the observed difference in protoxylem differentiation and the fact that a direct xylogenic effect of MeJA has been reported in the literature (Cenzano et al., 2003; Fattorini et al., 2009), it is reasonable to hypothesize a direct effect of MeJA on protoxylem differentiation, depending on H_2O_2 production via AtAO1 induction. The reduction of meristem size upon treatment with 50 μM MeJA could be mediated by the JA-induced repression of PLT1 and PLT2 expression, independently of the ROS distribution gradient, consistent with what was reported previously by Chen et al. (2011).

Put Supply or *AtAO1* Overexpression Induces Early Differentiation of Protoxylem Cells

PAs are well known to affect root development and xylem differentiation (Couée et al., 2004; Vera-Sirera et al., 2010). In this regard, PAs have been shown to alter root growth in a dose-dependent and tissue-specific manner by inducing or promoting cell division and/or expansion (Couée et al., 2004). Exogenous Spd has been shown to inhibit root growth in maize seedlings by reducing both the mitotic index and cell elongation as well as by altering cell cycle phase distribution in the root apex (de Agazio et al., 1995; Tisi et al., 2011b). In particular, PAO-mediated H_2O_2 production has been revealed to be a crucial player in the Spd-induced root

growth inhibition and early xylem differentiation observed in maize root (Tisi et al., 2011b). Here, we show that Put supply at the concentrations of 10 and 100 μM induced early protoxylem differentiation in wild-type but not in *Atao1* roots (Fig. 7; Supplemental Figs. S9 and S10) without impairing root growth (Fig. 7). These observations support the occurrence of a specific role of AtAO1-mediated Put catabolism in root protoxylem differentiation. Considering that acute stress, such as tip removal (de Agazio et al., 1992), similar to exogenous PAs (de Agazio et al., 1992; Tisi et al., 2011b; this work) or JA treatment (this work), results in early xylem differentiation, the hypothesis that PAs may behave as stress signaling compounds during root vascular differentiation could be formulated. Notably, the involvement of PAO and CuAO, respectively, in maize and Arabidopsis xylem differentiation highlights the complexity of PA catabolism, displaying different peculiarities depending on plant tissues and species. Interestingly, Put-induced protoxylem differentiation was fully reversed by DMTU treatment (Fig. 7; Supplemental Fig. S9), analogous to the MeJA-induced AtAO1-mediated effect on root xylem differentiation. Hence, the occurrence of a direct effect exclusively due to changes in Put levels can be excluded. Further support of a specific *AtAO1* involvement in Put-induced vascular differentiation in Arabidopsis is given by the absence of any selective effect of Spd on protoxylem differentiation in *Atao1* as compared with wild-type plants.

Consistent with our previous work on the effect of PA-derived H_2O_2 on xylem differentiation in transgenic tobacco plants overexpressing apoplastic ZmPAO (Tisi et al., 2011b), here we show that transgenic Arabidopsis plants overexpressing AtAO1 displayed (1) lower Put levels in roots (Fig. 8) as compared with the wild type, (2) early protoxylem differentiation (Fig. 8; Supplemental Fig. S12), and (3) a higher level of H_2O_2 at the site of the appearance of protoxylem cells with fully developed secondary wall deposition (Fig. 9). This added support to the hypothesis that PA-derived H_2O_2 could behave as a mediator in xylem tissue differentiation by contributing to the ROS gradient needed in the transition between cell proliferation and differentiation in the root meristem (Tsukagoshi et al., 2010). Indeed, an earlier protoxylem differentiation occurred in over*AtAO1* lines 3 and 11 (Fig. 8; Supplemental Fig. S12), which displayed a clearly visible accumulation of H_2O_2 in protoxylem cells about 630 and 570 μm from the root apex (Fig. 9) along with a marked decrease in Put levels (approximately 56%; Fig. 8), reasonably consequent to the high AtAO1 expression levels (Fig. 8).

In this regard, it has been hypothesized previously that both Spd supply and PAO overexpression may create an unphysiological environment in which a high rate of PA oxidation has been artificially forced to occur in the apoplast, hence simulating stress-like conditions (Tisi et al., 2011a). Furthermore, the absence of any defective phenotype in both antisense PAO tobacco plants (Tisi et al., 2011b) and *Atao1* mutants (this work) fails to unequivocally demonstrate the role of AOs in vascular development under physiological conditions. This would rather support the hypothesis that ROS signaling arising from oxidative PA catabolism is involved in the regulation of xylem differentiation during stress growth conditions, such as those simulated by (1) the high oxidation rate of PAs occurring in the apoplast upon their exogenous supply, (2) AO overexpression, or (3) MeJA treatments in a pathway independent of the cytokinin/auxin regulation loop (Perilli et al., 2012; Petricka et al., 2012).

MATERIALS AND METHODS

Plant Materials and Growth

The Columbia-0 (Col-0) ecotype of Arabidopsis (*Arabidopsis thaliana*) was used as the wild type. The Arabidopsis Col-0 T-DNA insertion lines *Atao1.1* (SALK_145639.55.25.X; TAIR accession no. 1005841762) and *Atao1.2* (SALK_077391.40.85.X; TAIR accession no. 4284859) of the *CuAO* gene At4g14940 (formerly *ATAO1* and referred to here as *AtAO1*; TAIR accession no. 2129519) were obtained from the SALK Institute Genomic Analysis Laboratory (http://signal.salk.edu/tabout.html; Alonso et al., 2003). Information on the T-DNA insertion mutants *Atao1.1* and *Atao1.2* was obtained from the SALK Institute Genomic Analysis Laboratory Web site (http://signal.salk.edu). The mutant *Atcoi1-16* and the corresponding wild type (Col gl1) were generous gifts of Alessandra Devoto. The Arabidopsis Col-0 transgenic lines (*AtAO1* promoter::*GFP-GUS* and constitutively expressing *AtAO1*) were constructed as reported below.

Plants were grown in soil and/or in vitro in a growth chamber at a temperature of 23°C under long-day conditions (16-/8-h photoperiod, 50 μmol m^{-2} s^{-1}, and 55% relative humidity). For in vitro growth, seeds were surface sterilized according to Valvekens et al. (1988). Seeds were cold stratified at 4°C and grown in one-half-strength Murashige and Skoog salt mixture supplemented with 0.5% (w/v) Suc in the presence or absence of 0.8% (w/v) agar. Seedlings grown in solid medium were kept in the vertical position to allow root growth on its surface.

For the analysis of *AtAO1* gene expression upon hormone treatment, 7-d-old Arabidopsis seedlings grown on agar medium were transferred to fresh medium alternatively containing 0.1 or 50 μM MeJA (from Duchefa), 100 μM ABA (from Duchefa), 10 μM NAA (from Sigma-Aldrich), or 1 μM BA (from Sigma-Aldrich). After 1-h (MeJA, NAA, and BA) or 2-h (ABA) treatments, total RNA was extracted as reported below.

For root xylem tissue and meristem analysis under LSCM or for PA extraction from root tissues upon Put or hormone treatment, the Arabidopsis wild type and *Atao1* mutants were treated as follows. Seven-day-old seedlings grown on agar medium were selected for root length homogeneity and transferred onto new medium alternately containing Put (1, 10, or 100 μM), Spd (10 μM), MeJA (0.1, 1, or 50 μM), ABA (0.1 or 1 μM), NAA (0.01, 0.1, or 1 μM), or BA (0.01, 0.1, or 1 μM). In the case of 10 μM Put and 0.1 μM MeJA, cotreatment with 100 μM DMTU was also analyzed. Plants were collected after 4 and 6 d for PA extraction and 7 d for the LSCM analysis. Alternatively, T2 seeds from *AtAO1*-overexpressing lines were grown for 7 d on selective medium and chosen for homogeneity of root length prior to being transferred to fresh plates. After an additional 11 d, plants were collected for PA extraction or LSCM analysis.

For histochemical GUS and GFP analysis by light microscopy or LSCM, 4-d-old seedlings grown on agar medium were transferred to fresh medium in the absence (control) or presence of 0.1 or 50 μM MeJA for 1 h.

Identification of the T-DNA Insertional Loss-of-Function *Atao1.1* and *Atao1.2* Mutants

Plants homozygous for the T-DNA insertion were identified by PCR on total DNA extracted from leaves by alkali treatment (Klimyuk et al., 1993) using gene- and T-DNA-specific primers. *AtAO1.1* and *AtAO1.2* gene-specifc primers (*RP-AtAO1.1*/*LP-AtAO1.1* and *RP-AtAO1.2*/*LP-AtAO1.2*) were designed outside of the 5′ and 3′ ends of the T-DNA insertion, and the T-DNA-specific primer (*LBa1*) was designed at its left border (Supplemental Fig. S1;

Supplemental Table S1). The genotype of the *Atao1* mutants was ascertained by two sets of PCR: one using *RP-AtAO1/LBa1* that determines the presence of the T-DNA insertion, and the other using *RP-AtAO1/LP-AtAO1* that verifies the absence of the fragment indicative of a wild-type allele, as the T-DNA insertion originates a nonamplifiable long transcript.

The presence of a single-locus T-DNA insertion in *Atao1.1* seedlings was analyzed by Southern blot, and the absence of the full-length *AtAO1* gene transcript in *Atao1.1* and *Atao1.2* seedlings was analyzed by RT-PCR of total RNA, using the gene-specific primers *rtAtAO1-for2* and *rtAtAO1-rev* (Supplemental Table S1).

For Southern-blot analysis, genomic DNA was purified from Arabidopsis seedlings as described by Fulton et al. (1995). Southern blotting was performed as described previously (Sambrook et al., 1989) after digestion with *Hin*dIII utilizing an insertion-specific probe. In particular, the fragments were detected by hybridization with a probe generated by PCR using the primers *T-test-for* and *T-test-rev* (Supplemental Table S1) for the promoter 35S region. PCR DIG Labeling Mix (Roche) was used to label the 560-bp Student's *t* test probe according to the manufacturer's procedures. The labeling of the probe was assessed as indicated in the protocol. Hybridization of the probe (10 μL of probe per 1 mL of hybridization solution) was performed using DIG Easy Hyb Granules (Roche) overnight at 42°C. Posthybridization washes of the nylon filter were performed using the DIG Wash and Block Buffer Set (Roche), and detection was performed using the DIG Luminescent Detection Kit (Roche) according to the manufacturer's procedures. The antibody was used at a dilution of 1:10,000 in blocking buffer.

Construction of *AtAO1* Promoter::*GFP-GUS* and Overexpressing Transgenic Lines

To construct *AtAO1*::*GFP-GUS* transgenic plants for *AtAO1*, a region of 2.6 kb upstream of ATG (herein named promoter *AtAO1*) was amplified from Arabidopsis Col-0 genomic DNA by PCR, cloned into the pDONR207 vector (Invitrogen) via Gateway technology (Invitrogen), and sequenced. The *AtAO1* promoter region was inserted upstream of the *GFP-GUS* fusion gene in the pKGWFS7 binary vector (Karimi et al., 2002). In particular, the promoter region of 2.6 kb was amplified for *AtAO1* using the oligonucleotides *PromAtAO1-for* and *PromAtAO1-rev* (Supplemental Table S1). The resulting *AtAO1*::*GFP-GUS* constructs were used to transform Arabidopsis Col-0 wild-type plants by the *Agrobacterium tumefaciens* (strain C58C1)-mediated floral dip transformation method as described (Clough and Bent, 1998). At least three independent transgenic lines, selected by kanamycin resistance and PCR analysis, at the T1, T2, and T3 generations, were examined for GUS and GFP activity.

The over*AtAO1* plants were prepared by Gateway technology. The *AtAO1* gene sequence was amplified by PCR from Arabidopsis genomic DNA using the gene-specific primers *overAtAO1-for* and *overAtAO1-rev* (Supplemental Table S1). The *overAtAO1-rev* primer was designed in order to insert the coding sequence for two Ser residues followed by a 6×His tag prior to the stop codon of the corresponding amplicon. The PCR product was purified and cloned initially into the pDONR 221 vector (Invitrogen), sequenced, and cloned into the pK2GW7 vector through the Gateway recombination system (Invitrogen). The pK2GW7 construct (*35SCaMV*::*AtAO1-6His*) was checked by sequencing prior to being transferred to *A. tumefaciens* (strain GV 301) and then used to transform Arabidopsis Col-0 wild-type plants by the floral dip transformation method (Clough and Bent, 1998). Putatively transformed plants were controlled on selective medium and subsequent PCR analysis of genomic DNA using the gene-specific primer *overAtAO1-for* and a 6×His tag-specific primer (Supplemental Table S1). Recombinant *AtAO1* expression in *35SCaMV*::*AtAO1-6His* transgenic plants was determined by RT-PCR using the gene-specific primer *rtAtAO1-for1* (Supplemental Table S1) and the 6×His tag-specific primer as well as western-blot analysis using a rabbit anti-6×His tag antibody conjugated to horseradish peroxidase (Abcam).

PCR, RT-PCR, and RT-qPCR Analysis

Total RNA was isolated either from rosette leaves of 30-d-old Arabidopsis plants or 7-d-old whole Arabidopsis seedlings using the RNeasy Plant Mini Kit (Qiagen) following the manufacturer's instructions. DNase digestion was performed during RNA purification using the RNase-Free DNase Set (Qiagen).

PCR was carried out with the DreamTaq DNA Polymerase (Fermentas) in an iCycler ThermalCycler (Bio-Rad) with the following parameters: 2 min of denaturation at 95°C; 35 cycles of 95°C for 30 s, 58°C for 1 min, and 72°C for 1.5 min; and 10 min at 72°C for a final extension. For RT-PCR, the first complementary DNA strand was synthesized from total RNA following the protocol of the ImProm-II Reverse Transcription System (Promega). *Ubiquitin5* (*UBQ5*) was used as an internal control to confirm equal amounts of RNA among the various samples, using the primers *UBQ5-for* and *UBQ5-rev* (Supplemental Table S1).

RT-qPCR analysis was performed on DNase-treated RNA (4 μg) from 7-d-old whole Arabidopsis seedlings. Complementary DNA synthesis and PCR amplification were carried out using GoTaq 2-Step RT-qPCR System200 (Promega) according to the manufacturer's protocol. The PCRs were run in a Corbett RG6000 device (Corbett Life Science, Qiagen) utilizing the following program: 95°C for 2 min, then 40 cycles of 95°C for 7 s and 60°C for 40 s. The melting program ramps from 60°C to 95°C, rising by 1°C each step. *AtAO1*-specific primers were *rtAtAO1-for2* and *rtAtAO1-rev* (Supplemental Table S1). *ACTIN8* (At1g49240) was used as a reference gene, and specific primers (*q-Actin8-for* and *qActin8-rev*) were prepared according to Hewezi et al. (2010; Supplemental Table S1). Fold change in the expression of *AtAO1* was calculated according to the $\Delta\Delta C_q$ method using the equation $\Delta\Delta C_q = 2^{-[\Delta Cq \text{ treated sample} - \Delta Cq \text{ control sample}]}$, with $\Delta C_q = C_{q \text{ target gene}} - C_{q \text{ reference gene}}$, where C_q refers to the quantification cycle (Livak and Schmittgen, 2001). The software used to control the thermocycler and to analyze data was the Corbett Rotor-Gene 6000 Application Software (version 1.7, build 87; Corbett Life Science, Qiagen).

Histochemical GUS and GFP Analysis

GUS staining of *AtAO1*::*GFP-GUS* Arabidopsis transgenic plants was performed essentially as described by Jefferson (1987). Briefly, seedlings were gently soaked in 90% (v/v) cold acetone for 1 h at −20°C for prefixation, rinsed with 50 mM sodium phosphate buffer at pH 7, and vacuum infiltrated in staining solution (1 mM 5-bromo-4-chloro-3-indolyl-β-D-glucuronide, 2.5 mM potassium ferrocyanide, 2.5 mM potassium ferricyanide, 0.2% [v/v] Triton X-100, 10 mM EDTA, and 50 mM sodium phosphate buffer, pH 7). The reaction was allowed to proceed at 37°C overnight or for 1 h in the case of MeJA treatments. Chlorophyll was extracted by several washings, first with ethanol: acetic acid (3:1) and then with 70% (v/v) ethanol. Images were acquired by a Leica DFC310FX digital camera applied to a Zeiss Axioplan2 microscope. GFP and PI (10 μg mL^{-1}; Sigma-Aldrich) fluorescence was analyzed using a laser scanning confocal microscope (Leica TCS-SP5 with the Leica Application Suite Advanced Fluorescence software) with an argon laser emitting at wavelength 488 nm and a selected emission band ranging from 505 to 560 nm for GFP and from 600 to 680 nm for PI. The images shown were obtained by aligning serial overlapping micrographs of the same root using Photoshop software (Adobe). To obtain transverse sections, GUS-stained seedlings were embedded in Technovit 7100 resin (Heraeus Kulzer), and 20-μm sections were obtained using a Microm HM330 microtome. Images were acquired with a Leica DFC420 digital camera applied to an Olympus BX51 microscope.

Cell Wall PI Staining, H_2O_2 in Situ Detection, and Bright-Field Analysis of Root Tissues

Arabidopsis root apices from 14-d-old seedlings of the wild type and the two *Atao1* mutants (control or treated with hormones, DMTU, or Put, for 7 d) as well as 18-d-old *AtAO1*-overexpressing transformed plants were incubated in 10 μg mL^{-1} PI for 5 min to reveal the outlines of cells as well as protoxylem (Mähönen et al., 2014) and then observed by LSCM using either a helium-neon laser emitting at wavelength 543 nm or an argon laser emitting at wavelength 488 nm using a 60× oil immersion objective or a 20× objective. The selected emission band ranged from 600 to 680 nm. During microscopic analysis, the staining reaction was allowed to proceed for the time needed to ensure PI penetration into the central cylinder, until the protoxylem staining was completed. In each examined root, the boundary between protoxylem cells with and without fully developed secondary cell wall thickenings was concurrently also analyzed by bright-field microscopy, using the same laser beam as described above. To determine the distance between protoxylem and apical meristem, the measurement was initiated from the position where a sharp intensification of protoxylem cell wall fluorescence after PI staining was detected, which is indicative of fully differentiated secondary cell wall thickenings (Fig. 4). The reported distances between protoxylem and apical meristem were validated by the correspondence between the site where fully developed secondary cell wall deposition was observed by bright-field microscopy analysis and the site where the sharp increase in the PI-induced fluorescence was revealed by LSCM. The length of the meristematic zone was

determined by measuring the distance between the quiescent center and the first elongating cell in the cortex cell file (Casamitjana-Martínez et al., 2003; Dello Ioio et al., 2008; Chen et al., 2011).

In situ detection of H_2O_2 in Arabidopsis roots was carried out by exploiting the fluorogenic peroxidase substrate AUR (Molecular Probes, Invitrogen), which reacts in a 1:1 stoichiometry with extracellular H_2O_2 (Ashtamker et al., 2007), producing a highly fluorescent reaction product (excitation/emission maxima of approximately 568/581 nm). Arabidopsis root apices, obtained from 14-d-old wild-type and *Atao1* seedlings (control or treated with MeJA for 7 d) as well as 18-d-old *AtAO1*-overexpressing transformed plants, were stained by incubation in 0.1 mM AUR for 5 or 10 min. After washing, root apices were observed by LSCM (helium-neon laser emitting at wavelength 543 nm). The selected emission band ranged from 550 to 700 nm. The micrographs shown are relative to the confocal central section of the root.

PA Quantification

Root free PA levels were determined in 11- and 13-d-old wild-type and the two *Atao1* mutant seedlings (untreated or treated with 0.1 or 50 μM MeJA for the last 4 or 6 d, respectively) and in 18-d-old over*AtAO1* plants.

The roots from at least 20 plants were separately pooled prior to being utilized. PAs were extracted overnight in 5% (w/v) perchloric acid (PCA) containing 0.15 mM 1,6-diaminohexane as an internal standard (tissue:5% PCA ratio of 1:3 [w/v]). The extracts were centrifuged at 20,000*g* for 15 min, and PCA-soluble free PAs were analyzed in the supernatant. A reference solution containing 1,3-diaminopropane, Put, 1,6-diaminohexane, Spd, and Spm was also prepared and treated as above to establish retention times and signal intensities for each compound during HPLC analysis.

PAs were quantified after derivatization with dansyl chloride according to Smith and Davies (1985) with minor modifications. Dansylated PAs were separated by HPLC (Agilent HPLC 1050 modules with diode array detector, model 1050, and fluorescence detector, model 1200) on a reverse-phase C18 column (Sperisorb S5 ODS2; 5-μm particle diameter, 4.6 × 250 mm) using a discontinuous solvent A (water:acetonitrile:methanol, 5:3:2) to solvent B (acetonitrile:methanol, 3:2) gradient elution (72% solvent A for 5 min; 72%–36% solvent A in 42 min; 36%–20% solvent A in 3 min; 20%–15% solvent A in 5 min; 15%–72% solvent A in 1 min; and 72% solvent A for 19 min, at a flow rate of 1 mL min^{-1}). The fluorescence detector was set at 365 and 510 nm for excitation and emission lights, respectively. The retention times were as follows: 1,3-diaminopropane, 17 min; Put, 18.7 min; 1,6-diaminohexane, 23.8 min; Spd, 37.1 min; and Spm, 51.6 min.

Statistics

The LSCM analysis after PI and AUR staining as well as the histochemical GUS and GFP analysis by light microscopy or LSCM were performed on five independent experiments on a minimum of five plants per genotype and per treatment, yielding reproducible results. Unless specified otherwise, SD was within 10% of the indicated values. Distance values between the first protoxylem cell with fully developed secondary cell wall thickenings and the apical meristem were measured after PI staining by LSCM, exploiting the Leica Application Suite Advanced Fluorescence software, and then used for statistical analysis. Images from single representative experiments are shown.

For the determination of soluble PA levels and RT-PCR analysis, at least three biological replicates were performed. For RT-qPCR analysis, two biological replicates each with three technical replicates were performed.

Statistical tests were performed using GraphPad Prism (GraphPad Software) with one-way ANOVA. The statistical significance of differences was evaluated by *P* levels as follows: ns, not significant; *, $P \leq 0.05$; **, $P \leq 0.01$; and ***, $P \leq 0.001$.

Sequence data from this article can be found in TAIR (http://www.arabidopsis.org) under accession numbers 2129519 (At4g14940; *AtAO1* gene), 1005841762 (Salk T-DNA insertional mutant line for the *AtAO1* gene; SALK_145639.55.25.X), and 4284859 (Salk T-DNA insertional mutant line for the *AtAO1* gene; SALK_077391.40.85.X).

Supplemental Data

The following supplemental materials are available.

Supplemental Figure S1. Characterization of the two T-DNA insertional mutants for *AtAO1* (TAIR accession no. 2129519).

Supplemental Figure S2. Nucleotide and deduced amino acid sequences of *AtAO1* retrieved from TAIR (TAIR accession no. 2129519).

Supplemental Figure S3. LSCM analysis after PI staining of root apices of 14-d-old wild-type Arabidopsis seedlings and respective bright-field image.

Supplemental Figure S4. LSCM analysis after PI staining of root apices of 14-d-old *Atao1.1* and *Atao1.2* Arabidopsis seedlings.

Supplemental Figure S5. Effects of MeJA and DMTU on root xylem differentiation in wild-type and *Atao1.1* Arabidopsis seedlings.

Supplemental Figure S6. Effect of ABA, cytokinin (BA), or auxin (NAA) on root growth, xylem differentiation, and *AtAO1* gene expression.

Supplemental Figure S7. In situ H_2O_2 detection by LSCM analysis after AUR staining and respective bright-field images of roots from the untreated wild type, untreated *Atao1*, and MeJA-treated *Atao1* mutants.

Supplemental Figure S8. Effect of MeJA treatment on Spd and Spm levels in roots of the wild type and *Atao1* mutants.

Supplemental Figure S9. Effect of exogenously supplied Put and/or DMTU on xylem differentiation in wild-type and *Atao1.1* Arabidopsis seedlings.

Supplemental Figure S10. Effect of MeJA and Put on root xylem differentiation in *Atao1.2* Arabidopsis seedlings.

Supplemental Figure S11. Spd and Spm levels expressed on a fresh weight (FW) basis in 18-d-old wild-type and over*AtAO1* roots.

Supplemental Figure S12. Effect of *AtAO1* overexpression on xylem differentiation.

Supplemental Figure S13. In situ H_2O_2 detection by LSCM analysis after AUR staining and respective bright-field image of roots from *AtAO1*-overexpressing seedlings, line 16.

Supplemental Table S1. Primers used in the PCR procedures.

ACKNOWLEDGMENTS

We thank M.M. Altamura (Università di Roma "La Sapienza") for helpful discussions, Dr. Pasquale Stano (Università degli Studi Roma Tre) for technical assistance with the HPLC analysis, the Arabidopsis Biological Resource Center for distributing the seeds of the SALK lines, and Alessandra Devoto (Royal Holloway University of London) for providing the *Atcoi1-16* seeds.

Received January 27, 2015; accepted April 15, 2015; published April 16, 2015.

LITERATURE CITED

Ahou A, Martignago D, Alabdallah O, Tavazza R, Stano P, Macone A, Pivato M, Masi A, Rambla JL, Vera-Sirera F, et al (2014) A plant spermine oxidase/dehydrogenase regulated by the proteasome and polyamines. J Exp Bot **65:** 1585–1603

Aloni R, Plotkin T (1985) Wound-induced and naturally occurring regenerative differentiation of xylem in *Zea mays* L. Planta **163:** 126–132

Alonso JM, Stepanova AN, Leisse TJ, Kim CJ, Chen H, Shinn P, Stevenson DK, Zimmerman J, Barajas P, Cheuk R, et al (2003) Genome-wide insertional mutagenesis of *Arabidopsis thaliana*. Science **301:** 653–657

Angelini R, Tisi A, Rea G, Chen MM, Botta M, Federico R, Cona A (2008) Involvement of polyamine oxidase in wound healing. Plant Physiol **146:** 162–177

Ashtamker C, Kiss V, Sagi M, Davydov O, Fluhr R (2007) Diverse subcellular locations of cryptogein-induced reactive oxygen species production in tobacco Bright Yellow-2 cells. Plant Physiol **143:** 1817–1826

Baayen RP (1986) Regeneration of vascular tissues in relation to Fusarium wilt resistance of carnation. Neth J Plant Pathol **92:** 273–285

Bishopp A, Help H, El-Showk S, Weijers D, Scheres B, Friml J, Benková E, Mähönen AP, Helariutta Y (2011) A mutually inhibitory interaction between auxin and cytokinin specifies vascular pattern in roots. Curr Biol **21:** 917–926

Boudart G, Jamet E, Rossignol M, Lafitte C, Borderies G, Jauneau A, Esquerré-Tugayé MT, Pont-Lezica R (2005) Cell wall proteins in apoplastic fluids of *Arabidopsis thaliana* rosettes: identification by mass spectrometry and bioinformatics. Proteomics **5:** 212–221

Casamitjana-Martínez E, Hofhuis HF, Xu J, Liu CM, Heidstra R, Scheres B (2003) Root-specific CLE19 overexpression and the sol1/2 suppressors implicate a CLV-like pathway in the control of Arabidopsis root meristem maintenance. Curr Biol **13:** 1435–1441

Cenzano A, Vigliocco A, Kraus T, Abdala G (2003) Exogenously applied jasmonic acid induces changes in apical meristem morphology of potato stolons. Ann Bot (Lond) **91:** 915–919

Chen Q, Sun J, Zhai Q, Zhou W, Qi L, Xu L, Wang B, Chen R, Jiang H, Qi J, et al (2011) The basic helix-loop-helix transcription factor MYC2 directly represses PLETHORA expression during jasmonate-mediated modulation of the root stem cell niche in *Arabidopsis*. Plant Cell **23:** 3335–3352

Clough SJ, Bent AF (1998) Floral dip: a simplified method for *Agrobacterium*-mediated transformation of *Arabidopsis thaliana*. Plant J **16:** 735–743

Cona A, Cenci F, Cervelli M, Federico R, Mariottini P, Moreno S, Angelini R (2003) Polyamine oxidase, a hydrogen peroxide-producing enzyme, is up-regulated by light and down-regulated by auxin in the outer tissues of the maize mesocotyl. Plant Physiol **131:** 803–813

Cona A, Rea G, Angelini R, Federico R, Tavladoraki P (2006) Functions of amine oxidases in plant development and defence. Trends Plant Sci **11:** 80–88

Couée I, Hummel I, Sulmon C, Gouesbet G, Amrani AEI (2004) Involvement of polyamines in root development. Plant Cell Tissue Organ Cult **76:** 1–10

Cui H, Hao Y, Kovtun M, Stolc V, Deng XW, Sakakibara H, Kojima M (2011) Genome-wide direct target analysis reveals a role for SHORT-ROOT in root vascular patterning through cytokinin homeostasis. Plant Physiol **157:** 1221–1231

de Agazio M, Federico R, Angelini R, De Cesare F, Grego S (1992) Spermidine pretreatment or root tip removal in maize seedlings: effects on K^+ uptake and tissue modifications. J Plant Physiol **140:** 741–746

de Agazio M, Grego S, Ciofi-Luzzatto A, Rea E, Zaccaria ML, Federico R (1995) Inhibition of maize primary root elongation by spermidine: effect on cell shape and mitotic index. J Plant Growth Regul **14:** 85–89

Dello Ioio R, Nakamura K, Moubayidin L, Perilli S, Taniguchi M, Morita MT, Aoyama T, Costantino P, Sabatini S (2008) A genetic framework for the control of cell division and differentiation in the root meristem. Science **322:** 1380–1384

Fattorini L, Falasca G, Kevers C, Rocca LM, Zadra C, Altamura MM (2009) Adventitious rooting is enhanced by methyl jasmonate in tobacco thin cell layers. Planta **231:** 155–168

Fincato P, Moschou PN, Spedaletti V, Tavazza R, Angelini R, Federico R, Roubelakis-Angelakis KA, Tavladoraki P (2011) Functional diversity inside the Arabidopsis polyamine oxidase gene family. J Exp Bot **62:** 1155–1168

Fulton TM, Chunwongse J, Tanksley SD (1995) Microprep protocol for extraction of DNA from tomato and other herbaceous plants. Plant Mol Biol Rep **13:** 207–209

Hewezi T, Howe PJ, Maier TR, Hussey RS, Mitchum MG, Davis EL, Baum TJ (2010) Arabidopsis spermidine synthase is targeted by an effector protein of the cyst nematode *Heterodera schachtii*. Plant Physiol **152:** 968–984

Hilal M, Zenoff AM, Ponessa G, Moreno H, Massa EM (1998) Saline stress alters the temporal patterns of xylem differentiation and alternative oxidase expression in developing soybean roots. Plant Physiol **117:** 695–701

Jefferson RA (1987) Assaying chimeric genes in plants: the GUS gene fusion system. Plant Mol Biol Rep **5:** 387–405

Karimi M, Inzé D, Depicker A (2002) GATEWAY vectors for Agrobacterium-mediated plant transformation. Trends Plant Sci **7:** 193–195

Kim DW, Watanabe K, Murayama C, Izawa S, Niitsu M, Michael AJ, Berberich T, Kusano T (2014) Polyamine Oxidase5 regulates Arabidopsis growth through thermospermine oxidase activity. Plant Physiol **165:** 1575–1590

Kim EH, Park SH, Kim JK (2009) Methyl jasmonate triggers loss of grain yield under drought stress. Plant Signal Behav **4:** 348–349

Klimyuk VI, Carroll BJ, Thomas CM, Jones JDG (1993) Alkali treatment for rapid preparation of plant material for reliable PCR analysis. Plant J **3:** 493–494

Lin CC, Kao CH (2001) Abscisic acid induced changes in cell wall peroxidase activity and hydrogen peroxide level in roots of rice seedlings. Plant Sci **160:** 323–329

Livak KJ, Schmittgen TD (2001) Analysis of relative gene expression data using real-time quantitative PCR and the $2^{(-\Delta\Delta C(T))}$ method. Methods **25:** 402–408

Mähönen AP, Bishopp A, Higuchi M, Nieminen KM, Kinoshita K, Törmäkangas K, Ikeda Y, Oka A, Kakimoto T, Helariutta Y (2006) Cytokinin signaling and its inhibitor AHP6 regulate cell fate during vascular development. Science **311:** 94–98

Mähönen AP, ten Tusscher K, Siligato R, Smetana O, Díaz-Triviño S, Salojärvi J, Wachsman G, Prasad K, Heidstra R, Scheres B (2014) PLETHORA gradient formation mechanism separates auxin responses. Nature **515:** 125–129

Mattoo AK, Minocha SC, Minocha R, Handa AK (2010) Polyamines and cellular metabolism in plants: transgenic approaches reveal different responses to diamine putrescine versus higher polyamines spermidine and spermine. Amino Acids **38:** 405–413

Møller SG, McPherson MJ (1998) Developmental expression and biochemical analysis of the *Arabidopsis atao1* gene encoding an H_2O_2-generating diamine oxidase. Plant J **13:** 781–791

Møller SG, Urwin PE, Atkinson HJ, McPherson MJ (1998) Nematode-induced expression of *atao1*, a gene encoding an extracellular diamine oxidase associated with developing vascular tissue. Physiol Mol Plant Pathol **53:** 73–79

Moschou PN, Paschalidis KA, Delis ID, Andriopoulou AH, Lagiotis GD, Yakoumakis DI, Roubelakis-Angelakis KA (2008) Spermidine exodus and oxidation in the apoplast induced by abiotic stress is responsible for H_2O_2 signatures that direct tolerance responses in tobacco. Plant Cell **20:** 1708–1724

Moschou PN, Sarris PF, Skandalis N, Andriopoulou AH, Paschalidis KA, Panopoulos NJ, Roubelakis-Angelakis KA (2009) Engineered polyamine catabolism preinduces tolerance of tobacco to bacteria and oomycetes. Plant Physiol **149:** 1970–1981

Munemasa S, Mori IC, Murata Y (2011) Methyl jasmonate signaling and signal crosstalk between methyl jasmonate and abscisic acid in guard cells. Plant Signal Behav **6:** 939–941

Murali Achary VM, Panda BB (2010) Aluminium-induced DNA damage and adaptive response to genotoxic stress in plant cells are mediated through reactive oxygen intermediates. Mutagenesis **25:** 201–209

Ohashi-Ito K, Fukuda H (2010) Transcriptional regulation of vascular cell fates. Curr Opin Plant Biol **13:** 670–676

Peña-Valdivia CB, Sánchez-Urdaneta AB (2009) Effects of substrate water potential in root growth of *Agave salmiana* Otto ex Salm-Dyck seedlings. Biol Res **42:** 239–248

Perilli S, Di Mambro R, Sabatini S (2012) Growth and development of the root apical meristem. Curr Opin Plant Biol **15:** 17–23

Petricka JJ, Winter CM, Benfey PN (2012) Control of *Arabidopsis* root development. Annu Rev Plant Biol **63:** 563–590

Planas-Portell J, Gallart M, Tiburcio AF, Altabella T (2013) Copper-containing amine oxidases contribute to terminal polyamine oxidation in peroxisomes and apoplast of Arabidopsis thaliana. BMC Plant Biol **13:** 109

Ren C, Han C, Peng W, Huang Y, Peng Z, Xiong X, Zhu Q, Gao B, Xie D (2009) A leaky mutation in *DWARF4* reveals an antagonistic role of brassinosteroid in the inhibition of root growth by jasmonate in Arabidopsis. Plant Physiol **151:** 1412–1420

Rost TL, Baum S (1988) On the correlation of primary root length, meristem size and protoxylem tracheary element position in pea seedlings. Am J Bot **75:** 414–424

Sambrook J, Fritsch EF, Maniatis T (1989) Molecular Cloning: A Laboratory Manual, Ed 2. Cold Spring Harbor Laboratory Press, Cold Spring Harbor, NY

Smith MA, Davies PJ (1985) Separation and quantitation of polyamines in plant tissue by high performance liquid chromatography of their dansyl derivatives. Plant Physiol **78:** 89–91

Swarbreck D, Wilks C, Lamesch P, Berardini TZ, Garcia-Hernandez M, Foerster H, Li D, Meyer T, Muller R, Ploetz L, et al (2008) The Arabidopsis Information Resource (TAIR): gene structure and function annotation. Nucleic Acids Res **36:** D1009–D1014

Tavladoraki P, Cona A, Federico R, Tempera G, Viceconte N, Saccoccio S, Battaglia V, Toninello A, Agostinelli E (2012) Polyamine catabolism: target for antiproliferative therapies in animals and stress tolerance strategies in plants. Amino Acids **42:** 411–426

Tisi A, Angelini R, Cona A (2011a) Does polyamine catabolism influence root development and xylem differentiation under stress conditions? Plant Signal Behav **6:** 1844–1847

Tisi A, Federico R, Moreno S, Lucretti S, Moschou PN, Roubelakis-Angelakis KA, Angelini R, Cona A (2011b) Perturbation of polyamine catabolism can strongly affect root development and xylem differentiation. Plant Physiol **157:** 200–215

Tsukagoshi H, Busch W, Benfey PN (2010) Transcriptional regulation of ROS controls transition from proliferation to differentiation in the root. Cell **143:** 606–616

Valvekens D, Montagu MV, Van Lijsebettens M (1988) Agrobacterium tumefaciens-mediated transformation of Arabidopsis thaliana root explants by using kanamycin selection. Proc Natl Acad Sci USA **85:** 5536–5540

Vera-Sirera F, Minguet EG, Singh SK, Ljung K, Tuominen H, Blázquez MA, Carbonell J (2010) Role of polyamines in plant vascular development. Plant Physiol Biochem **48:** 534–539

Wimalasekera R, Villar C, Begum T, Scherer GFE (2011) *COPPER AMINE OXIDASE1* (*CuAO1*) of *Arabidopsis thaliana* contributes to abscisic acid- and polyamine-induced nitric oxide biosynthesis and abscisic acid signal transduction. Mol Plant **4:** 663–678

Winter D, Vinegar B, Nahal H, Ammar R, Wilson GV, Provart NJ (2007) An "Electronic Fluorescent Pictograph" browser for exploring and analyzing large-scale biological data sets. PLoS ONE **2:** e718

Yamamoto R, Demura T, Fukuda H (1997) Brassinosteroids induce entry into the final stage of tracheary element differentiation in cultured *Zinnia* cells. Plant Cell Physiol **38:** 980–983